Per. Mineral. (2007), 76, 101-136
SPECIAL ISSUE: From Petrogenesis to Orogenesis
doi:10.2451/2007PM0011
http://go.to/permin

PERIODICO di MINERALOGIA
established in 1930

An International Journal of
MINERALOGY, CRYSTALLOGRAPHY, GEOCHEMISTRY, ORE DEPOSITS, PETROLOGY, VOLCANOLOGY
and applied topics on *Environment*, *Archaeometry* and *Cultural Heritage*

The Pliocene Montiferro volcanic complex (central-western Sardinia, Italy): geochemical observations and petrological implications

LORENZO FEDELE[1] *, MICHELE LUSTRINO[2, 3], LEONE MELLUSO[1], VINCENZO MORRA[1] and FOSCO D'AMELIO[1]

[1] Dipartimento di Scienze della Terra, Università di Napoli Federico II, via Mezzocannone 8, 80134, Napoli, Italy
[2] Dipartimento di Scienze della Terra, Università degli Studi di Roma La Sapienza, P.le Aldo Moro 5, 00185 Roma, Italy
[3] CNR-Istituto di Geologia Ambientale e Geoingegneria (IGAG), P.le Aldo Moro 5, 00185 Roma, Italy

Accepted, April 2007

ABSTRACT — The Montiferro volcanic complex is one of the several districts of Middle Miocene-Quaternary magmatism of Sardinia. It was active between 3.9 and 1.6 Ma, with a climax at 3.6 Ma. Erupted rocks have a wide spectrum of compositions, ranging from basic and ultrabasic to highly evolved lithotypes, belonging to three different magmatic suites: 1) strongly alkaline sodic series; 2) mildly alkaline sodic series; 3) tholeiitic series. The products of the strongly alkaline series are mainly basanites, erupted both at the first and at the last stages of Montiferro activity. Strongly alkaline magmas are likely to have risen rapidly to the surface, as testified by the common occurrence of mantle xenoliths and by the absence of differentiated products. The mildly alkaline series ranges from hawaiites to trachytes and phonolites through very abundant mugearites and few benmoreites. Primitive magmas of this series are likely to have ponded at crustal levels, experiencing both differentiation and crustal contamination processes. Finally, the tholeiitic series is mainly represented by rare basaltic andesites and a few basaltic trachyandesites straddling the alkaline/subalkaline boundary.

Incompatible trace elements, $^{87}Sr/^{86}Sr$ and $^{143}Nd/^{144}Nd$ isotopic ratios are consistent with the derivation of these products from a common mantle source, represented by a spinel-lherzolite. Primitive magmas of three magmatic suites may have generated by different degrees of partial melting of this source, progressively increasing from strongly alkaline (~1-3% partial melting) to mildly alkaline (~5-7%) and tholeiitic products (~10-12%). Geochemical modellings suggest that this source is represented by a DMM-like lithospheric mantle, metasomatised by small inputs of various crustal components.

RIASSUNTO — Il complesso vulcanico del Montiferro è uno dei numerosi distretti del magmatismo medio Miocenico-Quaternario della Sardegna. L'attività vulcanica abbraccia un intervallo di tempo compreso tra 3,9 e 1,6 Ma, con una fase di *climax* avvenuta intorno a 3,6 Ma. I campioni analizzati coprono un ampio spettro composizionale, comprendente prodotti da poco differenziati ad intermedi ed evoluti, appartenenti a tre diverse serie magmatiche: 1) serie sodica fortemente alcalina; 2) serie sodica moderatamente alcalina; 3) serie tholeiitica.

I prodotti della serie fortemente alcalina sono rappresentati principalmente da basaniti, messe in posto durante le fasi iniziali e finali di attività del Montiferro. La risalita in superficie di tali magmi sembra essere stata piuttosto rapida, come indicato dalla occasionale presenza di xenoliti di mantello e

* Corresponding author, E-mail: lofedele@unina.it

dall'assenza di prodotti differenziati. I prodotti della serie moderatamente alcalina vanno da hawaiiti a trachiti e fonoliti, attraverso termini intermedi rappresentati dai mugeariti (estremamente abbondanti) e benmoreiti (poco rappresentate). I magmi capostipite di questa serie hanno potuto ristagnare nella crosta, andando incontro a processi di differenziazione e contaminazione. Infine, i prodotti della serie subalcalina sono rappresentati principalmente da andesiti basaltiche e rare trachiandesiti basaltiche.

Le concentrazioni degli elementi incompatibili ed i rapporti isotopici di $^{87}Sr/^{86}Sr$ e $^{143}Nd/^{144}Nd$ suggeriscono una comune origine per i prodotti delle tre serie, la cui sorgente sarebbe rappresentata da una lherzolite a spinello. A partire da tale sorgente, i magmi primitivi si sarebbero originati per diversi gradi di fusione, progressivamente maggiori muovendo dai prodotti di serie fortemente alcalina (per una fusione parziale del ~1-3%) a quelli di serie moderatamente alcalina (~5-7%) fino a quelli di serie tholeiitica (~10-12%). Le modellizzazioni effettuate sulla base dei rapporti tra elementi incompatibili e dei rapporti isotopici indicano che la sorgente dei magmi del Montiferro è costituita da un mantello litosferico di tipo DMM, metasomatizzato attraverso l'introduzione di piccoli quantitativi di materiale di provenienza crostale.

Key words: *Sardinia, geochemistry, petrology, alkaline, tholeiitic*

Introduction

The Montiferro volcanic complex is one of the largest Middle Miocene-Quaternary volcanic districts of Sardinia, covering an area of ~400 km^2 in the central-western sector of the island (Fig. 1). The stratigraphic sequences of the Montiferro products have been studied in detail by several authors during the '70s (e.g., Beccaluva *et al.*, 1973; Deriu *et al.*, 1974a, 1974b; Gallo *et al.*, 1974; Assorgia *et al.*, 1976, 1978) up to the early '80s, when a geopetrographic map was published by Assorgia *et al.* (1981). Since then, after the work of Di Battistini *et al.* (1990), no more papers focusing on the Montiferro complex have been so far published, with the exception of a couple of papers (Montanini *et al.*, 1992; Montanini and Harlov, 2006) specifically dealing with the petrology of lower crust xenoliths within Montiferro lavas. This is unusual if compared to the wealth of data published in the last decade on various Middle Miocene-Quaternary Sardinian districts (e.g., Montanini *et al.*, 1994; Lustrino *et al.*, 1996, 2000, 2002, 2004, 2007a, 2007b; Gasperini *et al.*, 2000). This paper aims to fill the gap of petrological knowledge within the framework of the detailed characterisation of the most recent volcanic cycle of Sardinia, presenting new data for whole rock major and trace elements, mineral chemistry, Sr-Nd isotopic ratios and $^{40}Ar/^{39}Ar$ geochronology.

Geological background

During the last 30 Ma the entire circum-Mediterranean area has been characterised by a complex geotectonic evolution, which strongly influenced the magmatic activity of the area (e.g., Beccaluva *et al.*, 2007 and references therein; Lustrino and Wilson, 2007 and references therein). The large-scale tectonic evolution was mainly driven by the convergent movement of African and European plates in the Alpine orogeny framework (e.g., Ricou, 1994; Carminati *et al.*, 1998; Gueguen *et al.*, 1998; Mattei *et al.*, 2004).

Up to lower Oligocene times, Sardinia was part of the southern European continental margin (in spatial continuity with southern France). During Burdigalian the continental block of Sardinia and Corsica rotated counter-clockwise (Speranza *et al.*, 2002) and successively moved eastwards, determining the opening of the Ligurian-Provençal basin. These processes were related to the roll-back of an oceanic lithosphere slab, subducting towards NNW since late Oligocene times, whose hinge progressively drifted towards SE (Gueguen *et al.*, 1998; Gelabert *et al.*, 2002; Rosenbaum *et al.*, 2002; Speranza *et al.*, 2002; Mattei *et al.*, 2004; Langone *et al.*, 2006). Consequently, a magmatic cycle including calcalkaline and arc-tholeiitic products developed in the central-western part of the island approximately from 32 to 15 Ma (Lecca *et al.*, 1997; Lustrino *et al.*, 2004, and references therein).

After Langhian, the ongoing migration of the subduction hinge determined the opening of

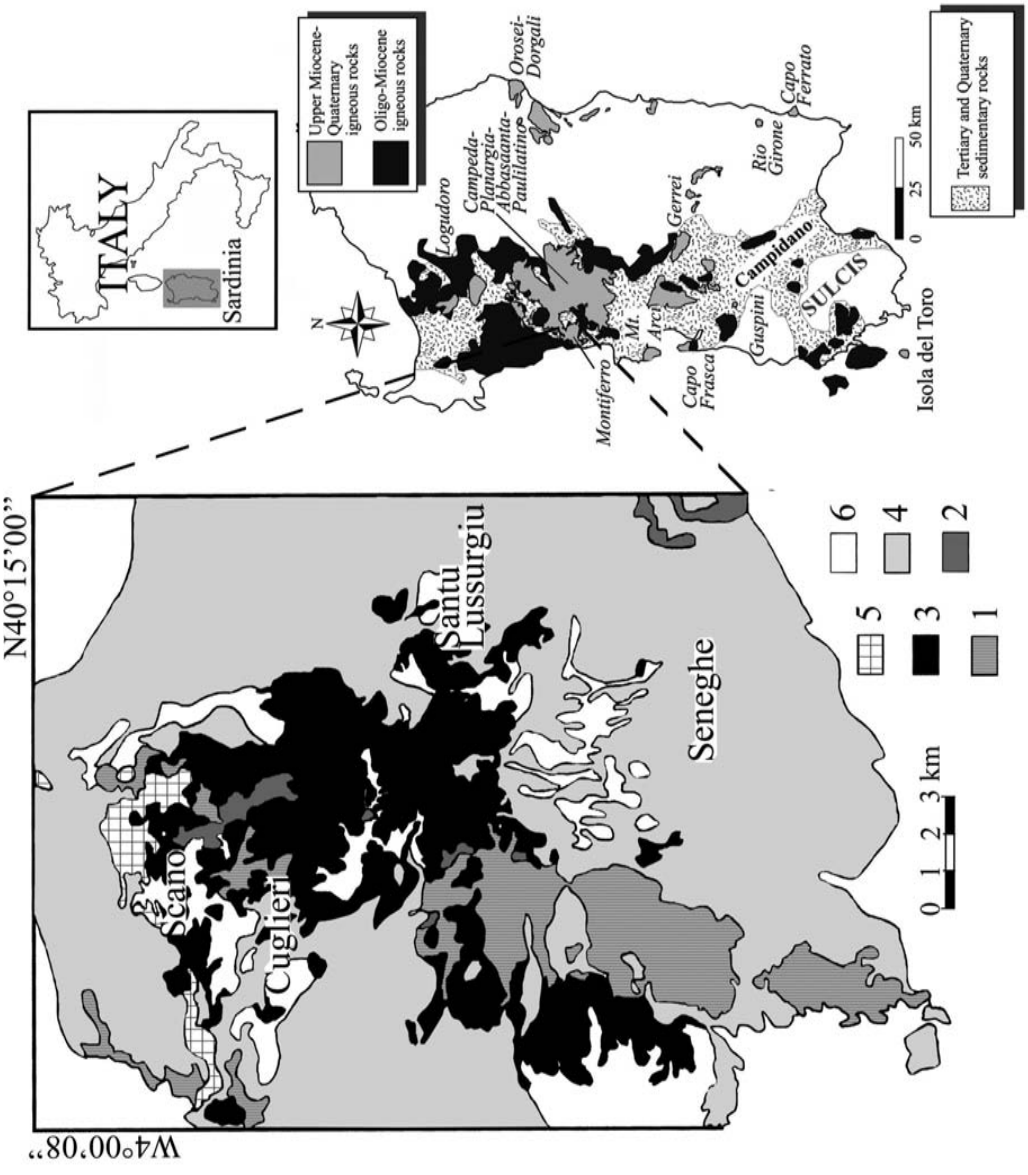

Fig. 1 – Geological sketch map of the Montiferro volcanic complex (modified from Assorgia *et al.*, 1981) and its localisation within Sardinia [modified from Lustrino *et al.* (2007b)]. 1 = Oligo-Miocene volcanic rocks; 2 = Lower Analcite Basanites (LAB) unit; 3 = Trachytes and Phonolites (TP) unit; 4 = Basalts and interlayered Differentiated rocks (BD) unit; 5 = Upper Analcite Basanites (UAB) unit; 6 = Quaternary sedimentary cover.

the Tyrrhenian back-arc basin (Gueguen *et al.*, 1998; Gelabert *et al.*, 2002; Rosenbaum *et al.*, 2002). The global extensional tectonic regime was active also in Sardinia where, during Middle Miocene-Quaternary, a new igneous episode developed throughout the island (e.g. Lustrino *et al.*, 2000, 2004, 2007a, 2007b). Middle Miocene-Quaternary volcanic rocks of Sardinia are represented by both alkaline and tholeiitic products, with geochemical features resembling magmas emplaced in within-plate tectonic settings, erupted within the time span ~11.8–0.1 Ma (Lustrino *et al.*, 2007b). Alkaline rocks are mainly represented by basic to intermediate compositions with mildly to strongly Na-alkaline affinities (mostly hawaiites and mugearites plus rarer basanites and alkali basalts), although some slightly potassic products have also been found (Lustrino *et al.*, 1996, 2004). Basic alkaline rocks commonly host ultramafic mantle xenoliths (Lustrino *et al.*, 1999, 2004; Beccaluva *et al.*, 2001) or, more rarely, lower crustal metagabbroic xenoliths (Montanini *et al.*, 1992; Montanini and Harlov, 2006). Tholeiitic rocks are mainly basaltic andesites plus rare tholeiitic basalts (Lustrino *et al.*, 1996, 2007a).

The Montiferro volcanic complex

The Pliocene Montiferro volcanic complex is located in central-western Sardinia (Fig. 1), at the intersection of two extensional fault systems: the NE-trending Marghine faults and the N-trending Campidano faults (Di Battistini *et al.*, 1990). The dominant structural features of the area seem to have deeply influenced the emplacement of the magmatic products, as shown by the orientation of dykes and the alignment of some necks and plugs (Deriu *et al.*, 1974a, Beccaluva *et al.*, 1983). Rock compositions span a very wide range, from ultrabasic to intermediate and evolved (i.e. basanites, hawaiites, mugearites, benmoreites, trachytes and phonolites).

Di Battistini *et al.* (1990) grouped the Montiferro products into four main volcanic units lying on a basement consisting of Oligo-Miocene volcanic rocks and Miocene shallow sea deposits (mainly limestones and sandstones). From bottom to top these eruptive sequences are:

Lower analcite basanites (LAB): this thin unit (maximum thickness 30 m; Gallo *et al.*, 1974) is represented by very small and scattered outcrops of few thin lava flows. The lower analcite basanites commonly host ultramafic (Beccaluva *et al.*, 2001) and gabbroic xenoliths (Assorgia *et al.*, 1981; Montanini and Harlov, 2006). K/Ar geochronology on plagioclases gave age values of ~3.9 Ma (Beccaluva *et al.*, 1985).

Trachytes and phonolites (TP): this unit represents the main body of the Montiferro complex, with lava flows and domes up to 300 m thick (Deriu, 1952, 1954; Brotzu *et al.*, 1970a, 1970b; Beccaluva *et al.*, 1973). These rocks, classified as tephritic phonolites to phonolites by Di Battistini *et al.* (1990), extensively outcrop in the central and northern sector of the edifice. K/Ar data performed on plagioclase separates gave age values ranging from 3.2 Ma (Beccaluva *et al.*, 1976-77) to 2.8 Ma (Coulon *et al.*, 1974).

Basalts and interlayered differentiated rocks (BD): the products of this sequence were erupted by several vents and small peripheral cones. Individual flow units are generally thin and deeply weathered. Anyway, flow units generally pile up reaching total thickness up to 300 m (Di Battistini *et al.*, 1990). Compositions range from alkali basalts to hawaiites, mugearites and benmoreites. Trachytes and trachyphonolites have also been found in the southern sector of the complex, where some tholeiitic basalts and basaltic andesites are intercalated with alkali basalts and hawaiites. Absolute age measurements on alkali basalt dykes gave values ranging between 3.1 and 2.3 Ma (K/Ar on plagioclases; Beccaluva *et al.*, 1983), while two lava flows have been dated respectively at 3.0 and 2.8 Ma (K/Ar on plagioclases; Beccaluva *et al.*, 1976-77).

Upper analcite basanites (UAB): the products of this unit are represented by very small and scarce outcrops (mainly in the northern part of the complex; Di Battistini *et al.*, 1990), in which the stratigraphic relations with the main trachyphonolitic body are not always very

TABLE 1

$^{40}Ar/^{39}Ar$ age measurements for Montiferro samples. Total fusion (TF), weighted plateau (plateau), normal isochron (normal) and inverse isochron (inverse) ages are reported in Ma, along with respective 2σ values. % ^{39}Ar, $^{40}Ar/^{36}Ar$ and $^{36}Ar/^{40}Ar$ values refer to plateau, normal isochron and inverse isochron age determinations, respectively. n.d. = not determined

Sample	Unit	TF	plateau	% ^{39}Ar	normal	$^{40}Ar/^{36}Ar$	inverse	$^{36}Ar/^{40}Ar$
GFP60	LAB	3.85 ± 0.04	3.86 ± 0.05	98.58	3.77 ± 0.09	394.4	3.77 ± 0.09	0.0025
GFP52	TP	3.59 ± 0.03	3.65 ± 0.03	88.26	3.70 ± 0.12	258.4	3.69 ± 0.12	0.0037
GFP69	BD	n.d.	3.14 ± 0.08	71.44	3.10 ± 0.16	365.3	3.11 ± 0.16	0.0032
GFP92	BD	3.79 ± 0.04	3.94 ± 0.54	61.37	2.42 ± 0.64	520.3	2.47 ± 0.61	0.0019

clear. Eruptive units occur as dykes, plugs and very small lava flows, ~1.6 Myr old (K/Ar on plagioclases; Assorgia *et al.*, 1981).

ANALYTICAL TECHNIQUES

$^{40}Ar/^{39}Ar$ step-heating and total fusion analyses were performed at the College of Oceanic and Atmospheric Sciences (COAS), Oregon State University (USA). Electron Micro Probe (EMP) analyses were carried out at the Istituto di Geologia Ambientale e Geoingegneria (IGAG), CNR, Rome (Italy), using a CAMECA SX50 electron microprobe with full WDS acquisition procedure. Data were reduced by using the PAP correction method. Whole rock major and trace elements were analyzed on pressed rock powder pellets by Philips PW1400 XRF spectrometer at the Centro Interdipartimentale di Servizio per Analisi Geomineralogiche (CISAG), Federico II University of Naples (Italy). Data were reduced following the method described by Melluso *et al.* (1997). Precision is better than 3% for major elements, 5% for Zn, Sr, Zr and Ba and better than 10% for the other trace elements. Na_2O and MgO were determined by Atomic Absorption Spectrophotometry (AAS) at the Dipartimento di Scienze della Terra of Naples (Italy). Precision is better than 2% for MgO and better than 6% for Na_2O. LOI (Loss On Ignition) was determined with standard gravimetric techniques after igniting rock powders at ~1000 °C for 4 hours. REEs and other trace elements were analyzed by ICP-MS at the Centre de Recherches Pétrographiques et Géochimiques (CRPG), Nancy (France). Uncertainties are typically within 5-10%. Sr and Nd isotope ratios were measured at the Dipartimento di Scienze della Terra of Florence (Italy) using a Finnigan TRITON TI mass spectrometer, following the procedure described by Avanzinelli *et al.* (2005). Repeated analyses of SRM 987 and La Jolla standards yielded values of $^{87}Sr/^{86}Sr = 0.710269 \pm 8$ (n = 17), and $^{143}Nd/^{144}Nd = 0.511844 \pm 7$ (n = 20). Total procedure blank for Sr was 40 pg.

$^{40}AR/^{39}AR$ GEOCHRONOLOGY

Absolute $^{40}Ar/^{39}Ar$ age measurements (Table 1) were performed on K-feldspar and plagioclase crystals separated from four samples, accurately chosen in order to be representative of the entire eruptive sequence recognised by Di Battistini *et al.* (1990). No age measurement was performed on samples belonging to the youngest UAB unit, given the deep alteration status of the samples.

Sample GFP60 (basanite) from the LAB unit gave a plateau age of 3.86 ± 0.05 Ma. Similar age values were obtained from the normal and inverse isochron methods (both 3.77 ± 0.09 Ma) and from the total fusion method (3.85 ± 0.04 Ma), thus confirming the reliability of the age measurement. There is a substantial consistency between the results of this study

and available literature K/Ar data for LAB unit (i.e., ~3.9 Ma; Beccaluva *et al.*, 1985). Sample GFP52 (phonolite), belonging to the TP unit, gave a plateau age of 3.65 ± 0.03 Ma, still in good agreement with normal isochron (3.70 ± 0.12 Ma), inverse isochron (3.69 ± 0.12 Ma) and total fusion (3.59 ± 0.03 Ma) ages. Previous K/Ar ages were significantly younger (i.e., ~3.2 Ma and ~2.8 Ma; Coulon *et al.*, 1974; Beccaluva *et al.*, 1976-77). Two samples were analyzed for the BD unit: mugearites GFP69 and GFP92. The first one yielded a plateau age of 3.14 ± 0.08 Ma, broadly confirmed by the similar normal and inverse isochron ages (3.10 ± 0.16 Ma and 3.11 ± 0.16 Ma, respectively). Sample GFP92, in contrast, did not yield any reliable plateau or isochron ages. Its total fusion age is 3.79 ± 0.04 Ma. This result is still highly debatable, given both the younger age data of 3.65 ± 0.03 Ma obtained for the underlying TP unit and the literature K/Ar data spanning from ~3.1 to ~2.3 Ma (Beccaluva *et al.*, 1976-77, 1985) for the products of BD unit.

Petrography

LAB unit. Most of the basanites are typically characterised by a low porphyricity index (hereafter P.I.; ~5%), with microlitic groundmass consisting of analcite, opaque oxides, olivine and altered glass. Clinopyroxene, anhedral olivine (commonly altered to iddingsite) and biotite are the main phenocryst phases; opaque oxides and analcite are present as microphenocrysts. Ultramafic spinel-lherzolite xenoliths, up to 12 cm in size, are also present. Few samples have higher P.I. (~20-25%), with olivine, clinopyroxene, amphibole (typically oxidised) and biotite phenocrysts, set up into a groundmass of analcite, olivine, plagioclase, opaque oxides and altered glass.

TP unit. Trachytes, trachyphonolites and phonolites have a typical fluidal "trachytic" texture, with alkali-feldspar (and, more rarely, clinopyroxene, plagioclase, amphibole and opaque oxides) phenocrysts set into a microlitic groundmass of iso-oriented alkali-feldspar, plagioclase, Ti-magnetite and sporadic clinopyroxene. Analcite crystals were found as groundmass microcrysts only within trachyphonolites and phonolites. Rare benmoreites were found in the lower part of this unit. The paragenesis consists of alkali-feldspar and minor clinopyroxene, amphibole, Ti-magnetite and biotite microphenocrysts. Groundmass is made up of feldspars, Ti-magnetite and sporadic analcite.

BD unit. Alkali basalts commonly show a P.I. ~25-30%, with variably altered (iddingsitised) olivine, clinopyroxene and sporadic plagioclase and magnetite phenocrysts, set up into a microlitic groundmass of plagioclase, olivine, clinopyroxene, opaque oxides and devitrified glass. Lherzolithic and gabbroic xenoliths (up to ~5 cm) rarely occur. Analcite was found as groundmass phase in a few samples, typically lacking plagioclase phenocrysts.

Hawaiites and mugearites widely outcrop in the Montiferro complex, and show a moderate porphyricity (P.I. ~15-20%), with plagioclase and minor olivine, clinopyroxene, amphibole, biotite and alkali-feldspar phenocrysts. Groundmass mainly consists of plagioclase, clinopyroxene, olivine, opaque oxides and analcite. Some orthopyroxene-bearing mugearites also occur, more properly referred to as basaltic trachyandesites (subalkaline affinity). Some samples also carry ultramafic and gabbroic xenoliths up to 4 cm in size. The rare benmoreites broadly show the same petrographic features previously reported for the benmoreites of the TP unit.

Finally, the rare tholeiitic rocks are represented by basaltic andesites with low P.I. (~5%). Phenocrysts are mainly plagioclases with sporadic olivine, set in a microlitic groundmass made of plagioclase, olivine, opaque oxides and clinopyroxene. The main petrographic difference between tholeiitic rocks and alkali basalts is the absence of clinopyroxene phenocrysts in the former.

UAB unit. Basanites belonging to this unit show many petrographic similarities with the basanites of the older LAB unit, i.e., low P.I. (~5%), clinopyroxene, olivine and biotite phenocrysts, sparse analcite and opaque oxides microcrysts and a microlitic

TABLE 2

Representative electron microprobe analyses of olivines of the Montiferro rocks. Oxides in wt.%. Structural formulas (a.p.f.u.) calculated on 4 oxygens. Fo % = forsterite mol.%. gm = groundmass; mpc = microphenocryst

sample	GFP51	GFP51	GFP51	GFP51	GFP92	GFP92	GFP92	GFP69	GFP69	GFP47	GFP55	GFP55	GFP55	GFP59	GFP59
point	core	rim	mpc	mpc	mpc	gm	core	mpc	gm	mpc	mpc	mpc	gm	mpc	core
SiO_2	40.63	41.06	40.73	40.75	38.64	37.57	39.43	37.09	36.04	39.68	39.59	39.65	34.02	39.80	39.64
FeO	12.05	11.08	11.81	12.82	24.15	26.08	19.90	30.98	38.06	17.15	18.13	17.53	45.15	17.76	19.51
MnO	0.19	0.11	0.12	0.12	0.29	0.45	0.22	0.39	0.54	0.13	0.20	0.24	0.62	0.21	0.23
MgO	45.13	46.38	48.22	47.35	36.52	34.31	40.09	31.27	25.94	41.71	41.55	42.09	20.09	40.97	40.51
CaO	0.10	0.13	0.14	0.14	0.17	0.23	0.14	0.23	0.11	0.21	0.22	0.21	0.33	0.23	0.21
Cr_2O_3	0.03	0.03	0.03	0.03		0.01			0.01	0.03	0.02	0.01	0.04	0.04	
NiO	0.43	0.26	0.37	0.33	0.08	0.20	0.23	0.07	0.08	0.21	0.20	0.37	0.09	0.33	0.24
Sum	98.57	99.05	101.42	101.54	99.85	98.85	100.01	100.03	100.76	99.11	99.90	100.11	100.34	99.34	100.35
Si	1.030	1.028	0.994	0.999	1.019	1.013	1.017	1.007	1.008	1.026	1.014	1.012	0.993	1.027	1.018
Fe^{2+}	0.255	0.232	0.241	0.263	0.533	0.588	0.429	0.704	0.891	0.348	0.388	0.374	1.103	0.383	0.419
Mn	0.004	0.002	0.002	0.002	0.006	0.010	0.005	0.009	0.013	0.003	0.004	0.005	0.015	0.005	0.005
Mg	1.705	1.731	1.755	1.730	1.436	1.379	1.542	1.266	1.082	1.609	1.586	1.601	0.875	1.576	1.550
Ca	0.003	0.003	0.004	0.004	0.005	0.007	0.004	0.007	0.003	0.007	0.006	0.006	0.010	0.006	0.006
Sum	2.997	2.997	2.997	2.998	2.998	2.997	2.997	2.993	2.997	2.992	2.997	2.998	2.997	2.997	2.998
Fo%	86.97	88.18	87.92	86.81	72.94	70.10	78.22	64.28	54.85	81.26	80.34	81.06	44.23	80.44	78.72

groundmass broadly consisting of the same phases. The two basanitic units are therefore indistinguishable on the basis of their petrographic features.

MINERAL CHEMISTRY

Olivine. Basanites are characterised by Mg-rich olivine with nearly uniform composition (Fo_{88-86}), whereas mugearites show a broader range of compositions (Fo_{80-55}), with Fe-rich olivine confined to the groundmass. With the exception of one Mg-poor (Fo_{44}) groundmass olivine, basaltic andesites also display constant and Mg-rich compositions (Fo_{84-80}). Geothermometric calculations indicate temperatures in the range 1140-1160 °C for basanites, 965-1090 °C for mugearites and 1040-1100 °C for basaltic andesites (Roeder and Emslie, 1970). Selected analyses of olivine are reported in Table 2.

Pyroxenes. Basanites host clinopyroxenes with augitic to salitic composition ($En_{40-34}Wo_{55-44}Fs_{13-8}$; Table 3) and slight chemical zoning. Ti spans a quite wide range, from 0.13 to 0.02 a.p.f.u., while Na ranges from 0.09 to 0.03 a.p.f.u.. Clinopyroxenes in mugearites are poorer in Ca and richer in Fe (augite; $En_{45-35}Wo_{44-40}Fs_{21-11}$), compared with those of basanites and generally display quite homogeneous unzoned compositions. Average Ti contents in clinopyroxenes of mugearites are significantly lower than those observed in the basanites (i.e., 0.05-0.01 a.p.f.u.). Clinopyroxenes in trachytes are salites with lower MgO ($En_{36-35}Wo_{48-47}Fs_{18-16}$) and higher Na (0.11-0.09 a.p.f.u.). Orthopyroxenes in BD basaltic andesites are Mg-richer ($En_{77-67}Wo_{3-2}Fs_{30-19}$) than those of basaltic trachyandesites ($En_{80}Wo_4Fs_{16}$; Table 3).

Table 3

Representative electron microprobe analyses of clinopyroxenes and orthopyroxenes of the Montiferro rocks. Oxides in wt.%. Structural formulas (a.p.f.u.) calculated on 6 oxygens. En % = enstatite mol.%; Wo % = wollastonite mol.%; Fs % = ferrosilite mol.%. gm = groundmass; mpc = microphenocryst

sample	GFP51						GFP92			GFP69			
point	rim	core	core	rim	gm	rim	core	rim	mpc	core	rim	rim	core
SiO_2	45.45	47.57	51.85	45.23	44.59	50.63	50.22	50.63	49.84	50.51	48.63	48.23	50.22
TiO_2	3.39	2.57	0.84	3.69	3.93	1.15	1.23	0.96	1.30	1.26	1.69	1.77	1.28
Al_2O_3	7.48	6.60	4.99	7.57	7.60	5.68	5.41	4.47	4.78	5.63	6.86	6.96	4.44
FeO	5.44	5.53	4.82	5.57	6.78	7.20	6.37	6.45	8.88	7.31	9.07	9.09	8.99
MnO	0.09	0.06	0.02	0.04	0.12	0.17	0.20	0.15	0.19	0.13	0.27	0.18	0.08
MgO	12.34	12.95	15.60	12.45	11.65	13.01	14.73	15.23	13.81	14.73	13.80	13.44	13.75
CaO	23.33	23.12	20.20	23.48	22.84	21.80	20.07	20.40	20.00	19.21	18.89	18.74	19.89
Na_2O	0.43	0.47	0.98	0.44	0.70	1.22	0.72	0.60	0.69	0.89	0.82	0.93	0.79
Cr_2O_3	0.61	0.58	0.05	0.48		0.01	0.51	0.58	0.03	0.31	0.09	0.08	0.14
Sum	98.57	99.43	99.34	98.94	98.20	100.87	99.45	99.44	99.51	99.97	100.12	99.41	99.58
Si	1.712	1.772	1.898	1.698	1.691	1.850	1.855	1.870	1.856	1.857	1.797	1.794	1.868
Ti	0.096	0.072	0.023	0.104	0.112	0.032	0.034	0.027	0.036	0.035	0.047	0.050	0.036
Al	0.332	0.290	0.215	0.335	0.340	0.245	0.236	0.194	0.210	0.244	0.299	0.305	0.195
Fe_{tot}	0.172	0.172	0.148	0.175	0.215	0.220	0.197	0.199	0.277	0.225	0.280	0.283	0.280
Mn	0.003	0.002	0.001	0.001	0.004	0.005	0.006	0.005	0.006	0.004	0.008	0.006	0.003
Mg	0.693	0.719	0.851	0.697	0.658	0.709	0.811	0.838	0.767	0.807	0.760	0.745	0.762
Ca	0.942	0.923	0.792	0.944	0.928	0.853	0.794	0.807	0.798	0.757	0.748	0.747	0.793
Na	0.032	0.034	0.070	0.032	0.051	0.086	0.051	0.043	0.050	0.063	0.059	0.067	0.057
Cr	0.018	0.017	0.001	0.014	0.000	0.000	0.015	0.017	0.001	0.009	0.003	0.002	0.004
Sum	4.000	4.000	4.000	4.000	4.000	4.000	4.000	4.000	4.000	4.000	4.000	3.999	3.998
En %	38.31	39.61	47.52	38.34	36.47	39.65	44.85	45.34	41.50	45.02	42.31	41.85	41.49
Wo %	52.05	50.81	44.22	51.98	51.41	47.75	43.92	43.65	43.21	42.22	41.63	41.95	43.16
Fs %	9.64	9.58	8.26	9.68	12.12	12.60	11.23	11.01	15.29	12.76	16.07	16.20	15.36

TABLE 3 — *continued...*

GFP69			GFP52		GFP59			GFP69		GFP55	GFP59	
rim	core	rim	rim	rim	gm	core	rim	rim	core	mpc	rim	core
50.30	49.67	51.09	49.87	50.45	51.71	51.48	50.33	54.16	54.18	54.99	53.05	53.19
1.53	1.28	1.29	1.61	1.19	1.22	0.34	1.41	0.21	0.39	0.26	0.30	0.25
3.38	4.97	2.17	3.32	3.10	1.77	2.09	3.51	2.71	3.09	3.19	2.90	2.35
8.56	8.85	8.71	9.59	8.58	9.99	12.55	8.19	13.25	11.97	10.26	18.81	18.66
0.15	0.21	0.19	0.99	0.89	0.24	0.34	0.16	0.22	0.14	0.13	0.37	0.22
14.36	14.35	14.33	11.43	11.98	15.20	11.79	14.27	27.06	27.28	28.95	23.68	23.94
21.00	18.70	21.11	21.47	22.31	19.40	21.00	20.62	1.73	1.71	1.85	1.30	1.07
0.49	0.82	0.40	1.45	1.21	0.41	0.37	0.46	0.11	0.15	0.09	0.15	0.07
0.02	0.05	0.05	0.03		0.06		0.23	0.42	0.48	0.59	0.08	0.05
99.77	98.89	99.34	99.76	99.71	99.99	99.96	99.18	99.88	99.39	100.32	100.61	99.79
1.870	1.854	1.912	1.869	1.885	1.923	1.947	1.882	1.942	1.945	1.939	1.933	1.953
0.043	0.036	0.036	0.045	0.033	0.034	0.010	0.040	0.006	0.011	0.007	0.008	0.007
0.148	0.219	0.096	0.146	0.136	0.077	0.093	0.155	0.115	0.131	0.133	0.124	0.101
0.266	0.276	0.273	0.301	0.268	0.311	0.397	0.256	0.397	0.359	0.303	0.573	0.573
0.005	0.007	0.006	0.032	0.028	0.007	0.011	0.005	0.007	0.004	0.004	0.011	0.007
0.796	0.798	0.799	0.639	0.667	0.843	0.664	0.795	1.447	1.460	1.522	1.286	1.310
0.837	0.748	0.846	0.862	0.893	0.773	0.851	0.826	0.066	0.066	0.070	0.051	0.042
0.035	0.059	0.029	0.105	0.088	0.030	0.027	0.034	0.008	0.011	0.006	0.010	0.005
0.000	0.001	0.001	0.001	0.000	0.002	0.000	0.007	0.012	0.014	0.017	0.002	0.002
3.999	3.999	3.999	4.000	4.000	4.000	4.000	3.999	4.000	4.000	4.000	3.999	4.000
41.80	43.64	41.54	34.84	35.93	43.57	34.55	42.24	75.46	77.28	80.17	66.94	67.81
43.96	40.88	43.98	47.03	48.11	39.98	44.24	43.88	3.46	3.47	3.68	2.63	2.17
14.24	15.47	14.48	18.12	15.96	16.46	21.21	13.87	21.08	19.24	16.15	30.42	30.02

Table 4

Representative electron microprobe analyses of plagioclases and alkali-feldspars of the Montiferro rocks. Oxides in wt.%. Structural formulas (a.p.f.u.) calculated on 8 oxygens. An % = anorthite mol.%; Or % = orthoclase mol.%; Ab % = albite mol.%. gm = groundmass; mpc = microphenocryst

sample	GFP92					GFP69					
point	mpc	rim	core	rim	core	gm	core	rim	core	rim	gm
SiO_2	56.31	54.44	57.15	54.80	57.47	54.30	57.08	54.34	56.03	55.83	56.11
TiO_2	0.12	0.11	0.08	0.11	0.07	0.12	0.10	0.08	0.10	0.07	0.13
Al_2O_3	27.47	28.38	26.83	28.24	26.30	28.04	26.72	27.88	26.85	27.27	26.97
FeO	0.45	0.55	0.46	0.55	0.44	0.65	0.51	0.65	0.50	0.51	0.71
MgO	0.04	0.06	0.04	0.05	0.04	0.06	0.04	0.05	0.05	0.04	0.04
CaO	9.71	11.27	9.21	10.91	8.60	11.61	9.25	11.01	9.55	9.97	10.07
Na_2O	5.56	4.94	5.71	4.94	6.08	4.78	5.56	4.96	5.61	5.50	5.45
K_2O	0.85	0.63	1.04	0.62	0.99	0.51	1.03	0.54	0.90	0.77	0.61
Sum	100.51	100.36	100.51	100.23	99.99	100.06	100.29	99.51	99.58	99.96	100.09
Si	2.528	2.454	2.562	2.475	2.584	2.461	2.569	2.472	2.537	2.520	2.534
Al	1.454	1.508	1.418	1.504	1.394	1.498	1.418	1.494	1.433	1.450	1.436
Fe^{3+}	0.017	0.021	0.017	0.021	0.017	0.025	0.019	0.025	0.019	0.019	0.027
Ca	0.467	0.544	0.442	0.528	0.414	0.564	0.446	0.537	0.463	0.482	0.487
Na	0.483	0.432	0.496	0.433	0.530	0.420	0.485	0.438	0.492	0.481	0.477
K	0.049	0.036	0.060	0.035	0.057	0.029	0.059	0.031	0.052	0.044	0.035
Sum	4.997	4.995	4.995	4.996	4.996	4.996	4.996	4.996	4.997	4.997	4.997
An %	48.39	42.66	49.70	43.43	52.94	41.47	49.01	43.51	48.87	47.78	47.73
Or %	4.87	3.55	5.98	3.56	5.67	2.90	5.97	3.13	5.13	4.39	3.53
Ab %	46.74	53.79	44.32	53.01	41.38	55.62	45.02	53.36	45.99	47.83	48.75

Plagioclase. Mugearites are characterised by labradoritic to andesinic plagioclase ($An_{56-41}Ab_{53-41}Or_{6-3}$), showing both normal and inverse zoning. Tholeiitic samples of the BD unit (basaltic andesites) show a significantly wider spectrum (i.e., $An_{61-28}Ab_{68-40}Or_{4-1}$). Representative analyses of plagioclases are reported in Table 4.

Alkali-feldspar. Sanidine was found only in trachytes and phonolites and shows little compositional variability (i.e., $Ab_{58-51}Or_{46-37}An_{3-5}$; Table 4).

Opaque oxides. Opaque crystals are mainly Ti-magnetites with quite variable TiO_2 contents (ulvospinel contents ranging from 63 to 26%; Table 5), decreasing from basanites to trachytes. Sporadic rhombohedral phases (TiO_2 ~46 wt.%; ilmenite content ~88%) were found in mugearites. Geothermobarometric calculations [Spencer and Lindsley (1981); Andersen and Lindsley (1985)] on coexisting magnetite and ilmenite crystals yielded temperature estimates of ~785-820 °C and oxygen fugacity (fO_2) estimates of ~10^{-13} bar (ΔQFM ranging from -2.5 to -1.3).

Biotite. Biotite (in mugearites) has Mg# ~81, Al ~1.64 a.p.f.u., Fe ~0.85 a.p.f.u., and K ~1.38 a.p.f.u. (not shown).

Major and trace elements

Ninety-nine Montiferro samples were analyzed for major and trace elements. Representative analyses are reported in Table 6; the complete list can be requested to the first author.

TABLE 4 — *continued...*

GFP47			GFP55						GFP59			GFP52		
gm	core	rim	core	rim	gm	core	rim	gm	core	rim	gm	mpc	mpc	mpc
54.40	54.22	53.98	53.58	58.56	54.62	52.57	55.69	62.79	55.47	57.06	55.50	66.31	66.37	66.50
0.10	0.02	0.10	0.05	0.13	0.10	0.04	0.06	0.14	0.18	0.12	0.12	0.10	0.01	
28.44	28.51	28.25	28.40	25.65	28.36	28.97	27.37	23.11	27.29	26.34	27.29	19.74	19.67	19.32
0.69	0.67	0.57	0.50	0.54	0.68	0.52	0.55	0.71	0.99	0.80	1.12	0.32	0.24	0.11
0.16	0.28	0.13	0.16	0.09	0.16	0.14	0.12	0.05	0.18	0.11	0.13			
11.64	11.86	11.57	12.17	8.40	11.79	12.76	10.72	5.77	10.69	9.26	10.75	1.01	1.07	0.60
4.82	4.49	5.09	4.50	6.63	4.84	4.32	5.34	7.75	5.27	6.05	5.12	6.61	6.46	5.82
0.22	0.24	0.25	0.22	0.51	0.23	0.18	0.28	0.75	0.59	0.59	0.56	6.38	7.08	7.97
100.47	100.29	99.93	99.58	100.51	100.76	99.50	100.13	101.06	100.65	100.32	100.58	100.47	100.91	100.32
2.454	2.453	2.442	2.440	2.617	2.457	2.397	2.513	2.781	2.494	2.563	2.500	2.962	2.951	2.982
1.512	1.520	1.506	1.524	1.351	1.503	1.557	1.456	1.206	1.446	1.394	1.449	1.039	1.031	1.021
0.026	0.026	0.021	0.019	0.020	0.026	0.020	0.021	0.026	0.037	0.030	0.042	0.012	0.009	0.004
0.563	0.575	0.561	0.594	0.402	0.568	0.623	0.518	0.274	0.515	0.446	0.519	0.048	0.051	0.029
0.422	0.394	0.446	0.397	0.574	0.422	0.382	0.467	0.666	0.460	0.527	0.447	0.572	0.557	0.506
0.013	0.014	0.015	0.013	0.029	0.013	0.011	0.016	0.042	0.034	0.034	0.032	0.363	0.402	0.456
4.990	4.981	4.991	4.988	4.992	4.990	4.990	4.992	4.996	4.985	4.993	4.989	4.997	5.000	4.998
42.29	40.06	43.67	39.58	57.11	42.07	37.59	46.62	67.83	45.60	52.35	44.78	58.15	55.16	51.07
1.29	1.42	1.43	1.29	2.86	1.33	1.05	1.62	4.29	3.34	3.35	3.23	36.92	39.77	46.04
56.42	58.51	54.90	59.13	40.03	56.60	61.36	51.76	27.87	51.06	44.30	51.99	4.93	5.07	2.89

TABLE 5.

Representative electron microprobe analyses of opaque oxides of the Montiferro rocks. Oxides in wt.%. Ulvospinel (Usp %) and ilmenite (Ilm %) mol.% were calculated according to the methods of Lindsay and Spencer (1982) and Stormer (1983). gm = groundmass; mpc = microphenocryst

sample	GFP51	GFP59	GFP92	GFP69	GFP52	GFP69
point	gm	gm	mpc	mpc	mpc	mpc
TiO_2	16.33	20.46	15.80	8.30	9.39	46.40
Al_2O_3	3.80	1.36	7.31	9.25	0.98	0.13
FeO	68.92	70.43	68.58	67.93	79.70	44.89
MnO	0.59	0.41	0.39	0.30	2.95	0.46
MgO	4.51	0.79	4.60	6.16	0.57	3.95
Cr_2O_3	0.88	0.02	0.02	2.00		0.17
NiO	0.14	0.03	0.11	0.22		
Sum	95.17	93.50	96.82	94.16	93.58	96.00
Usp%	49.05	62.62	52.25	28.49	26.25	
Ilm%						87.62

Table 6 — *Major elements (wt.%), LOI (wt.%), trace elements (ppm), and CIPW norm (restricted output) of representative Montiferro rock samples. Major elements concentrations were recalculated to LOI-free basis. Mg# = Mg/(Mg+Fe^{2+}); ΔQ = qz-ne. AB = alkali basalt; bA = basaltic andesite; Ben = benmoreite; Bsn = basanite; bTA = basaltic trachyandesite; Haw = hawaiite; Mug = mugearite; P = phonolite; T = trachyte. b.d.l. = below detection limit*

Label	GFP44	GFP51	GFP64	FDP48	GFP73	GFP62	FDP1	FDP2	GFP45	GFP46	GFP66	GFP81	GFP86	GFP83
Unit	UAB	UAB	UAB	LAB	BD	UAB	LAB	LAB	BD	BD	BD	BD	BD	BD
Rock type (TAS)	Bsn	Bsn	Bsn	AB	Haw	Haw	Mug	Mug	Mug	Mug	Mug	Mug	Mug	Mug
SiO_2	44.76	47.39	46.15	47.16	50.55	50.30	51.47	53.17	52.65	53.42	52.59	53.90	54.20	50.03
TiO_2	3.10	3.09	3.02	3.64	2.03	3.24	2.09	2.09	1.80	1.97	1.86	2.08	2.96	2.08
Al_2O_3	13.29	13.41	13.69	13.10	15.00	13.86	14.24	15.66	15.06	15.00	15.37	15.71	16.43	14.36
Fe_2O_3	10.52	10.01	9.77	11.26	10.56	10.21	10.23	9.12	10.62	10.90	10.32	9.34	11.97	10.41
MnO	0.15	0.14	0.14	0.15	0.14	0.14	0.13	0.11	0.13	0.12	0.13	0.12	0.14	0.14
MgO	11.83	10.07	11.43	8.80	7.38	7.35	9.03	5.01	6.06	5.04	5.79	4.44	1.93	8.47
CaO	9.02	8.28	8.76	9.55	7.77	8.02	6.27	6.72	7.58	7.09	7.37	6.06	3.90	7.35
Na_2O	5.51	5.42	5.27	4.17	3.66	4.30	3.61	5.14	4.15	4.06	4.10	4.56	4.14	4.09
K_2O	0.93	1.32	0.90	0.82	2.28	1.79	2.26	2.31	1.56	1.92	1.98	3.18	3.58	2.58
P_2O_5	0.89	0.87	0.87	1.35	0.63	0.79	0.68	0.68	0.39	0.48	0.49	0.62	0.74	0.50
LOI	1.78	2.90	2.03	3.55	0.13	3.94	1.10	1.46	0.60	0.80	0.04	0.03	2.53	0.11
Na_2O/K_2O	5.91	4.11	5.85	5.10	1.61	2.41	1.60	2.23	2.65	2.11	2.07	1.43	1.16	1.59
Mg#	0.72	0.70	0.73	0.65	0.62	0.63	0.67	0.56	0.57	0.52	0.57	0.53	0.27	0.66
Zn	88	77	90	83	93	94	87	75	100	107	99	102	145	96
Ni	291	265	278	154	186	135	105	98	136	143	113	96	15	254
Rb	121	41	104	135	45	92	29	11	23	38	38	62	62	49
Sr	1037	1084	1057	812	793	835	805	911	604	675	608	810	700	796
Y	22	23	22	22	35	26	14	16	16	25	20	25	38	19
Zr	333	353	322	281	194	202	205	181	156	167	193	311	303	215
Nb	68	76	78	48	38	53	43	41	24	28	29	46	54	43
Sc	23	16	22	24	19	19	15	15	20	17	16	17	11	18
V	229	255	217	317	183	250	156	154	164	171	171	149	183	173
Cr	535	414	464	261	274	278	165	205	285	271	235	126	9	368
Ba	1740	2127	1670	2625	1169	1377	1097	1362	631	823	732	1164	1409	1148
CIPW norm														
qz	0.0	0.0	0.0	0.0	0.0	0.0	0.0	0.0	0.0	0.0	0.0	0.0	2.4	0.0
or	5.5	7.8	5.3	4.8	13.4	10.6	13.4	13.6	9.2	11.4	11.7	18.8	21.2	15.2
ab	13.5	22.2	19.2	29.2	30.1	33.1	30.5	39.3	35.1	34.3	34.7	38.5	35.0	25.0
an	8.8	8.3	11.1	14.6	17.8	13.2	16.0	12.8	17.8	17.0	17.7	13.0	14.5	13.2
ne	17.9	12.9	13.8	3.3	0.4	1.8	0.0	2.3	0.0	0.0	0.0	0.0	0.0	5.2
di	24.1	21.6	21.3	19.3	13.6	17.3	8.6	13.1	14.1	12.4	12.8	10.6	0.0	16.2
hy	0.0	0.0	0.0	0.0	0.0	0.0	9.0	0.0	8.4	15.1	6.6	0.5	15.5	0.0
ol	19.0	16.3	18.6	15.3	16.1	12.9	13.8	10.5	7.8	1.7	8.6	10.3	0.0	16.9
mt	2.3	2.2	2.2	2.5	2.3	2.3	2.3	2.0	2.3	2.4	2.3	2.1	2.6	2.3
il	5.9	5.9	5.7	6.9	3.9	6.2	4.0	4.0	3.4	3.7	3.5	4.0	5.6	4.0
ΔQ	-17.9	-12.9	-13.8	-3.3	-0.4	-1.8	0.0	-2.3	0.0	0.0	0.0	0.0	2.4	-5.2

TABLE 6 — *continued...*

GFP92	GFP94	GFP96	FDP14	FDP17	FDP19	FDP21	FDP22	FDP23	FDP26	FDP43	FDP54	GFP65	GFP57	FDP28	FDP44
BD	BD	BD	BD	BD	BD	BD	BD	BD	BD	BD	BD	UAB	BD	BD	BD
Mug	Mug	Mug	Mug	Mug	Mug	Mug	Mug	Mug	Mug	Mug	Mug	Mug	Ben	Ben	Ben
51.77	53.75	53.13	52.98	53.50	53.71	52.19	53.03	51.18	53.83	50.37	52.76	51.16	55.28	58.60	54.59
2.29	1.98	1.82	1.97	1.69	1.90	2.06	2.06	2.08	1.97	2.12	2.46	1.93	1.93	1.30	1.94
14.97	15.05	14.85	17.64	16.62	15.50	14.36	15.62	15.15	15.59	16.42	14.98	15.68	16.96	17.69	16.72
10.38	10.82	10.44	8.91	8.86	9.03	10.05	8.95	10.90	9.57	9.59	11.27	9.89	8.45	6.44	8.31
0.13	0.11	0.13	0.12	0.12	0.12	0.13	0.11	0.15	0.13	0.14	0.10	0.13	0.11	0.09	0.11
6.09	4.55	6.43	3.62	4.51	5.65	8.37	5.10	6.28	4.74	5.56	3.84	6.39	3.26	1.06	3.38
6.75	6.96	6.96	6.91	6.68	6.12	5.97	6.86	7.29	5.87	7.41	7.37	7.51	5.31	3.00	5.39
3.89	4.09	4.07	4.17	4.36	4.09	3.61	5.49	4.86	4.13	5.14	3.75	4.47	3.65	5.32	4.66
2.79	2.25	1.83	2.95	2.63	3.03	2.59	2.10	1.36	3.16	2.18	2.57	2.22	4.18	5.14	3.58
0.94	0.42	0.34	0.73	1.02	0.84	0.66	0.68	0.77	1.00	1.06	0.89	0.61	0.86	1.36	1.32
0.37	1.16	0.33	0.42	0.61	0.19	2.89	0.12	1.57	0.76	0.60	1.13	1.35	0.89	0.75	0.38
1.39	1.81	2.23	1.41	1.65	1.35	1.39	2.62	3.58	1.30	2.36	1.46	2.01	0.87	1.04	1.30
0.58	0.50	0.59	0.49	0.54	0.59	0.66	0.57	0.57	0.54	0.58	0.44	0.60	0.47	0.28	0.49
101	111	116	76	82	93	84	77	99	97	85	102	89	87	88	82
118	134	141	23	96	111	90	102	161	117	100	144	149	55	b.d.l.	61
50	43	33	44	49	56	45	11	12	55	68	43	41	76	107	70
925	721	646	690	666	801	776	907	802	839	823	844	713	906	541	753
16	26	18	18	15	17	17	19	17	25	20	21	22	22	23	18
190	198	176	175	169	203	212	179	161	213	248	140	173	288	383	222
37	31	23	36	30	40	41	42	38	40	49	33	32	48	55	38
18	15	13	16	12	16	12	14	20	14	17	20	15	9	7	7
185	165	153	172	142	147	147	153	192	155	188	198	170	132	54	128
182	226	222	26	157	189	153	206	239	204	145	273	258	61	b.d.l.	73
1384	1196	694	1050	912	1129	1074	1352	1166	1275	1156	1173	962	1712	1644	1385
0.0	0.0	0.0	0.0	0.0	0.0	0.0	0.0	0.0	0.0	0.0	0.4	0.0	1.4	1.0	0.0
16.5	13.3	10.8	17.4	15.6	17.9	15.3	12.4	8.0	18.7	12.9	15.2	13.1	24.7	30.4	21.2
32.9	34.6	34.5	35.3	36.9	34.6	30.6	38.9	38.6	34.9	31.8	31.7	31.6	30.9	45.0	39.4
15.2	16.1	16.8	20.7	18.0	15.0	15.3	11.8	15.5	14.7	15.3	16.5	16.1	17.5	6.0	14.1
0.0	0.0	0.0	0.0	0.0	0.0	0.0	4.1	1.3	0.0	6.4	0.0	3.4	0.0	0.0	0.0
9.9	13.0	12.6	7.2	6.9	8.0	8.0	14.5	12.7	6.5	11.9	11.9	13.9	2.6	0.0	3.3
4.7	13.1	10.9	4.0	8.3	9.2	10.8	0.0	0.0	11.9	0.0	14.1	0.0	14.6	8.9	8.0
11.2	1.9	6.9	7.2	6.0	6.9	11.4	10.1	14.7	4.3	12.4	0.0	13.7	0.0	0.0	4.7
2.3	2.4	2.3	2.0	2.0	2.0	2.2	2.0	2.4	2.1	2.1	2.5	2.2	1.9	1.4	1.8
4.4	3.8	3.4	3.7	3.2	3.6	3.9	3.9	3.9	3.7	4.0	4.7	3.7	3.7	2.5	3.7
0.0	0.0	0.0	0.0	0.0	0.0	0.0	-4.1	-1.3	0.0	-6.4	0.4	-3.4	1.4	1.0	0.0

Table 6 — *continued...*

Label	GFP89	GFP90	GFP93	FDP51	GFP87	GFP88	GFP68	GFP42	GFP52	GFP91	FDP47	FDP50	GFP48
Unit	TP	TP	TP	TP	BD	BD	TP	TP	TP	TP	TP	TP	BD
Rock type (TAS)	T	T	T	T	T	T	P	P	P	P	P	P	P
SiO_2	58.85	58.74	60.82	62.40	60.37	61.34	61.26	59.72	61.08	60.05	60.97	60.22	60.36
TiO_2	1.12	1.10	0.83	0.52	0.71	0.62	0.60	0.36	0.46	0.56	0.52	0.75	0.81
Al_2O_3	19.65	19.84	19.51	19.93	20.54	19.91	19.92	20.35	19.86	21.27	19.94	19.81	19.34
Fe_2O_3	4.57	4.36	3.33	2.84	3.30	2.49	2.73	2.38	2.34	2.60	2.30	2.68	3.20
MnO	0.14	0.12	0.14	0.15	0.15	0.13	0.15	0.17	0.16	0.13	0.14	0.13	0.14
MgO	0.89	0.90	0.52	0.37	0.51	0.29	0.06	0.34	0.38	0.29	0.21	0.56	0.55
CaO	3.26	3.62	1.81	1.46	1.77	1.65	1.54	1.37	1.56	1.93	1.44	2.04	1.98
Na_2O	5.74	5.47	5.29	5.24	5.14	6.01	6.33	7.70	6.86	5.38	7.15	5.67	5.70
K_2O	5.47	5.49	7.64	6.85	7.39	7.50	7.35	7.58	7.21	7.72	7.23	7.99	7.77
P_2O_5	0.30	0.36	0.12	0.25	0.12	0.06	0.07	0.03	0.08	0.07	0.10	0.16	0.15
LOI	2.66	3.00	1.75	1.31	2.34	1.22	0.91	1.38	1.15	3.72	0.56	1.15	0.74
Na_2O/K_2O	1.05	1.00	0.69	0.76	0.70	0.80	0.86	1.02	0.95	0.70	0.99	0.71	0.73
Mg#	0.31	0.32	0.27	0.23	0.26	0.21	0.05	0.25	0.28	0.20	0.17	0.33	0.28
Zn	67	61	73	69	80	63	75	77	70	64	65	60	76
Ni	1	3	b.d.l.	3	b.d.l.	5	1	3	3	3	1	b.d.l.	5
Rb	168	187	129	129	105	159	146	169	164	181	142	104	130
Sr	1396	1367	142	88	121	115	76	129	57	297	56	214	334
Y	26	27	31	28	29	31	20	26	28	28	23	31	40
Zr	611	583	697	751	750	870	914	1143	966	1013	842	696	831
Nb	94	87	120	109	132	136	124	131	120	139	103	113	114
Sc	4	1	1	2	2	b.d.l.	2	b.d.l.	2	b.d.l.	1	b.d.l.	5
V	45	49	33	18	28	28	27	18	24	31	22	33	34
Cr	b.d.l.	b.d.l.	b.d.l.	b.d.l.	b.d.l.	b.d.l.	b.d.l.	b.d.l.	b.d.l.	b.d.l.	b.d.l.	b.d.l.	b.d.l.
Ba	884	847	50	484	13	21	25	9	b.d.l.	38	5	28	56
CIPW norm													
qz	0.0	0.0	0.0	1.3	0.0	0.0	0.0	0.0	0.0	0.0	0.0	0.0	0.0
or	32.4	32.4	45.1	40.5	43.7	44.3	43.4	44.8	42.6	45.6	42.7	47.2	45.9
ab	42.1	41.6	36.7	44.3	38.2	37.4	37.9	27.4	36.6	33.5	36.1	31.0	33.1
an	11.7	13.4	6.9	5.6	8.0	5.2	4.2	0.0	2.1	9.1	1.0	5.0	4.2
ne	3.5	2.5	4.4	0.0	2.9	7.3	8.5	19.0	11.6	6.5	13.2	9.2	8.2
di	2.1	1.9	1.1	0.0	0.0	2.2	2.7	5.7	4.4	0.0	4.8	3.4	3.9
hy	0.0	0.0	0.0	3.9	0.0	0.0	0.0	0.0	0.0	0.0	0.0	0.0	0.0
ol	4.0	3.9	2.9	0.0	3.4	1.5	1.2	0.7	0.9	2.5	0.3	1.6	1.8
mt	1.0	1.0	0.7	0.6	0.7	0.6	0.6	0.0	0.5	0.6	0.5	0.6	0.7
il	2.1	2.1	1.6	1.0	1.4	1.2	1.1	0.7	0.9	1.1	1.0	1.4	1.5
ΔQ	-3.5	-2.5	-4.4	1.3	-2.9	-7.3	-8.5	-19.0	-11.6	-6.5	-13.2	-9.2	-8.2

TABLE 6 — *continued...*

GFP50	GFP47	GFP55	FDP57	FDP3	GFP43	GFP53	GFP56	GFP58	Label
TP	BD	BD	BD	TP	BD	BD	BD	BD	Unit
bA	bA	bA	bA	bTA	bTA	bTA	bTA	bTA	Rock type (TAS)
54.03	52.87	53.80	55.27	53.63	53.18	54.62	53.29	54.12	SiO_2
1.79	1.66	1.62	1.63	1.90	1.80	1.99	2.19	1.77	TiO_2
15.15	14.57	15.95	15.73	15.08	15.71	14.66	14.83	15.11	Al_2O_3
10.07	11.11	10.34	10.10	10.63	10.06	11.51	11.02	10.92	Fe_2O_3
0.12	0.16	0.13	0.13	0.12	0.12	0.10	0.11	0.15	MnO
5.36	7.17	5.46	4.72	5.61	4.69	3.78	5.44	4.91	MgO
8.37	7.78	7.58	6.89	7.40	7.62	7.36	6.91	7.23	CaO
3.49	3.30	3.88	4.44	4.11	4.50	3.78	3.40	3.76	Na_2O
1.28	1.15	1.03	0.66	1.26	1.77	1.90	2.30	1.70	K_2O
0.33	0.22	0.22	0.44	0.27	0.55	0.31	0.48	0.32	P_2O_5
0.89	0.67	0.44	0.32	0.06	0.10	1.76	1.20	0.99	LOI
2.73	2.87	3.78	6.76	3.26	2.55	1.99	1.48	2.21	Na_2O/K_2O
0.55	0.60	0.55	0.52	0.55	0.52	0.43	0.54	0.51	Mg#
98	105	96	108	96	91	129	137	109	Zn
121	169	213	137	108	90	122	150	150	Ni
24	22	25	12	91	29	32	36	37	Rb
520	537	490	629	542	667	661	748	613	Sr
20	18	17	16	b.d.l.	22	20	20	21	Y
126	120	111	74	100	148	172	202	151	Zr
19	17	16	12	20	20	27	31	24	Nb
15	17	16	14	15	17	16	16	16	Sc
166	168	151	136	174	163	163	175	161	V
209	262	228	262	228	173	225	221	221	Cr
467	472	407	457	523	741	665	925	664	Ba
									CIPW norm
3.0	0.6	1.5	3.9	0.0	0.0	3.3	1.0	1.8	qz
7.6	6.8	6.1	3.9	7.4	10.4	11.2	13.6	10.1	or
29.6	27.9	32.8	37.5	34.8	38.1	32.0	28.8	31.8	ab
21.9	21.6	23.1	21.1	19.0	17.4	17.4	18.4	19.3	an
0.0	0.0	0.0	0.0	0.0	0.0	0.0	0.0	0.0	ne
14.4	12.7	10.7	8.4	13.1	13.8	14.2	10.5	11.9	di
16.4	23.4	19.1	18.0	18.2	5.7	13.9	19.0	17.6	hy
0.0	0.0	0.0	0.0	0.0	6.8	0.0	0.0	0.0	ol
2.2	2.5	2.3	2.2	2.4	2.2	2.5	2.4	2.4	mt
3.4	3.2	3.1	3.1	3.6	3.4	3.8	4.2	3.4	il
3.0	0.6	1.5	3.9	0.0	0.0	3.3	1.0	1.8	ΔQ

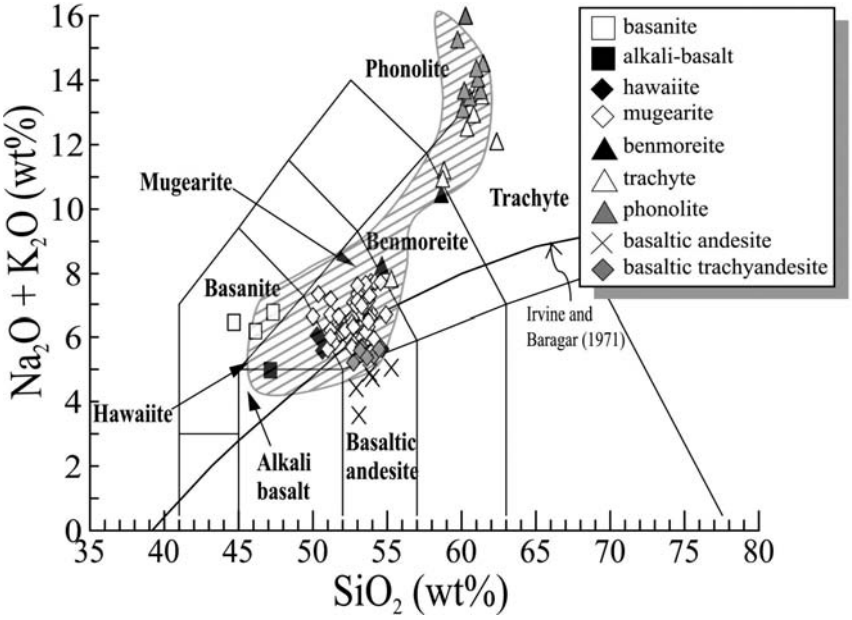

Fig. 2 – TAS classification diagram (Le Bas *et al.*, 1986) for the Montiferro samples. Gray-striped area represents the composition of literature data for Montiferro rocks (Beccaluva *et al.*, 1973a; Deriu *et al.*, 1974a; Di Battistini *et al.*, 1990; Godano, 2000; Lustrino *et al.*, 2000, 2007a). The thick curved line represents the limit between alkaline and subalkaline compositions (Irvine and Baragar, 1971).

According to the TAS classification scheme (Le Bas *et al.*, 1986; Fig. 2), samples are mainly mugearites. More primitive (i.e., basanites, hawaiites and alkali basalts) and more evolved rocks (benmoreites, trachytes and phonolites) are subordinate. Tholeiitic samples also occur, represented by few basaltic andesites and opx-bearing, CIPW quartz-normative, basaltic trachyandesites.

Major and trace elements vs. MgO diagrams are reported in Fig. 3 and Fig. 4. Basanites and alkali basalts have the highest MgO (11.8-8.8 wt.%), CaO (9.5-8.3 wt.%) and TiO_2 (3.6-3.0 wt.%) and the lowest SiO_2 (44.8-50.6 wt.%), Al_2O_3 (13.7-13.1 wt.%) and K_2O (together with basaltic andesites and basaltic trachyandesites; 0.8-1.3 wt.%). Basanites and alkali basalts have a variably SiO_2-undersatured character (ΔQ from –13 to –18 in the basanites and around –3 in the alkali basalts; ΔQ represents the amount of CIPW-normative quartz minus CIPW-normative nepheline and leucite), generally coupled with the highest Na_2O/K_2O ratios (4.1-5.9).

Hawaiites and mugearites are characterised by a wide range of MgO (i.e., from 9.3 to 1.9 wt.%). Similar wide ranges are observed for Al_2O_3 (from 13.7 to 17.6 wt.%), CaO (8.3-3.9 wt.%), Na_2O (3.0-5.7 wt.%) and K_2O (1.1-3.6 wt.%). Na_2O/K_2O ratios are high and variable (~1.2-4.1), whereas ΔQ is typically around 0, with few samples showing lower values (from –1.3 up to –6.3). Intermediate lithotypes also include few tholeiitic, SiO_2-satured to SiO_2-oversatured (i.e., $\Delta Q = 0$ and $\Delta Q = 0.4$-3.8, respectively) basaltic andesites (MgO ~8.0-4.7 wt.%) and basaltic trachyandesites (MgO ~6.4-3.8 wt.%), with typically lower TiO_2, K_2O and Na_2O and higher CaO with respect to their alkaline (mugearitic) counterparts at a given MgO content (Table 6).

The most evolved rocks of Montiferro are mainly trachytes and phonolites, showing the highest SiO_2, Na_2O, K_2O, and the lowest TiO_2, Fe_2O_3 and CaO (Table 6). Few benmoreites (from BD unit) also occur, showing intermediate compositions between mugearites and the trachytes/phonolites group.

As regards trace elements, basanites have higher incompatible element contents (e.g., Rb 41-135 ppm, Zr 280-350 ppm, Nb 48-76 ppm, Ba 1740-

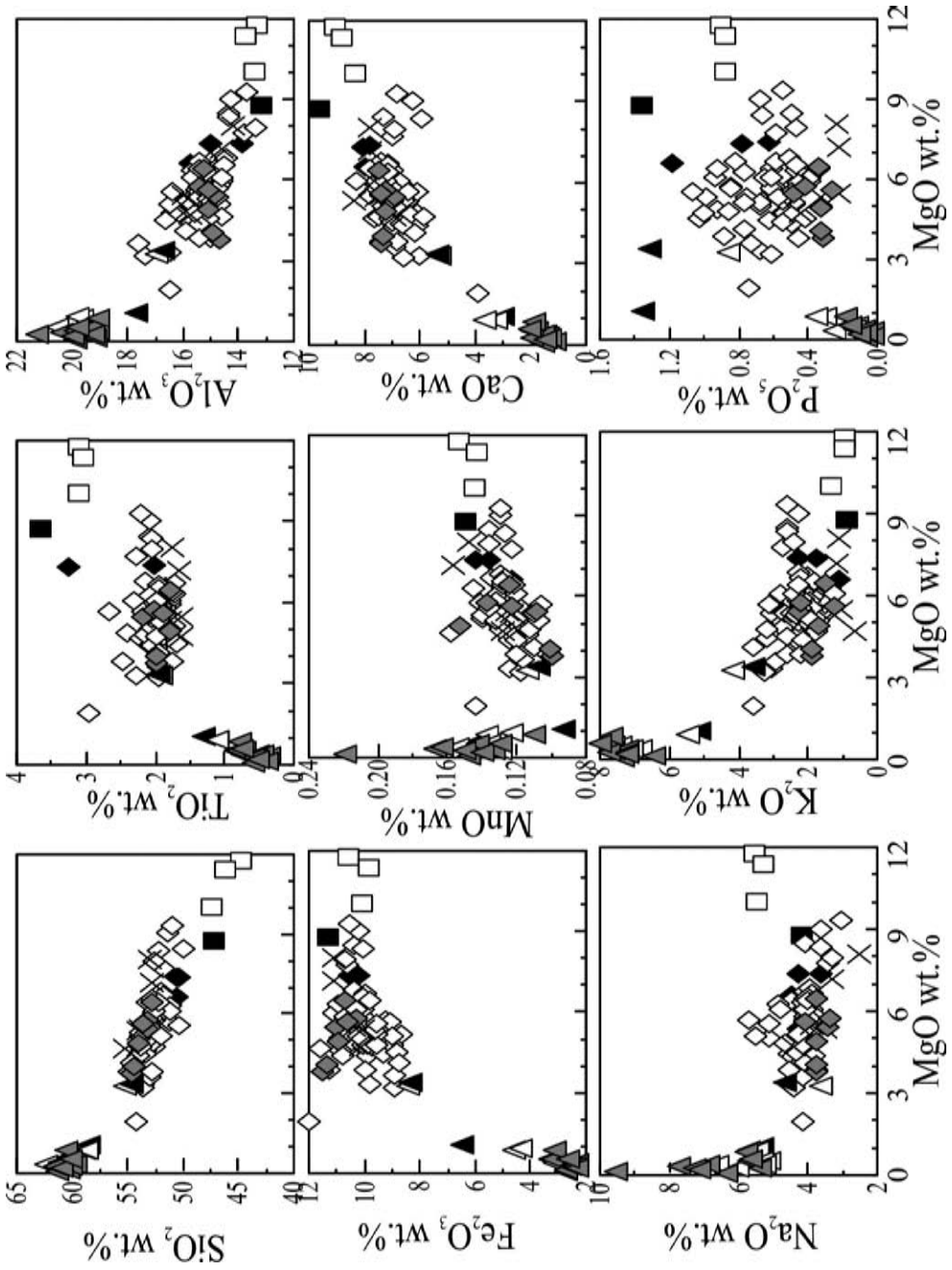

Fig. 3 – Major elements binary variation diagrams for the Montiferro samples. Symbols as in Fig. 2.

2625 ppm) with respect to hawaiites and mugearites (e.g., Rb 10-90 ppm, Zr 100-300 ppm, Nb 10-50 ppm, Ba 1410-690 ppm). With the only exception of Ba, the highest incompatible element contents (e.g., Nb ~85-150 ppm, Rb ~100-220 ppm, Zr ~580-1100 ppm) are observed in the most evolved Montiferro products (Tables 6-7). On the other hand, strongly compatible trace elements show a general good positive correlation with MgO, with the highest values observed for basanites and alkali basalts (e.g., Sc 24-16 ppm, V 317-175 ppm, Ni 290-135 ppm, Cr 535-260 ppm) and a quite constant decrease moving to hawaiites and mugearites (Sc 22-15 ppm, V 250-150 ppm, Ni 250-15 ppm, Cr 370-10 ppm), up to benmoreites, trachytes and phonolites (Sc <10 ppm, V 130-17 ppm, Ni <55 ppm, Cr <70 ppm). Subalkaline rocks have trace element ranges broadly similar to alkaline intermediate rocks, with tendentially lower incompatible element contents at a given MgO (e.g., Zr 74-202 ppm, Nb 12-36 ppm, Ba 925-410 ppm).

A selection of Montiferro samples was chosen for ICP-MS trace element analyses (Table 7). Primitive mantle-normalised multielemental patterns of the most primitive Montiferro rocks are quite smooth, with positive peaks at Ba, Pb and P and small troughs at Th, K and Nb (Fig. 5), resembling magmas emplaced in within-plate tectonic settings, with no HFSE (High Field Strength Elements) troughs and normalised abundances decreasing almost uniformly from La to Y. The peak at Ba is a typical feature of Middle Miocene-Quaternary rocks from Sardinia (e.g., Cioni *et al.*, 1982; Di Battistini *et al.*, 1990; Lustrino *et al.*, 1996, 2000, 2002, 2004, 2007a; Gasperini *et al.*, 2000; Beccaluva *et al.*, 2005). Basanites (from both LAB and UAB units) show strong incompatible element (e.g., LREE, Rb,

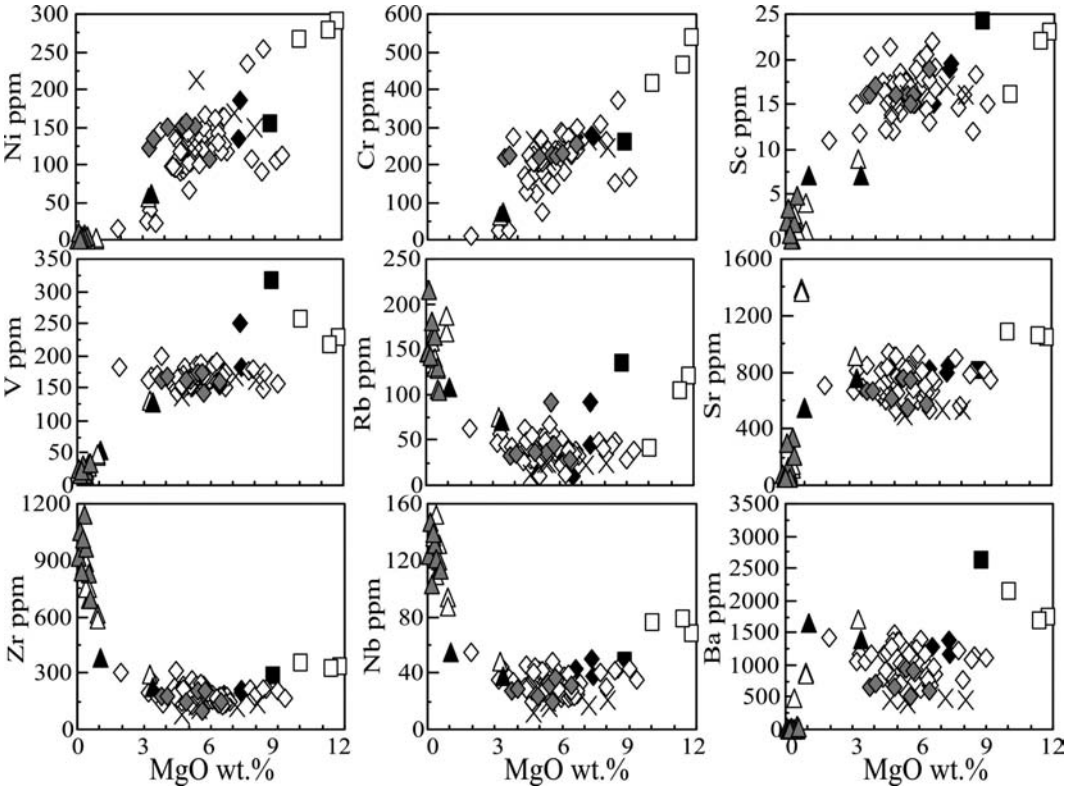

Fig. 4 – Selected trace elements binary variation diagrams for the Montiferro samples. Symbols as in Fig. 2.

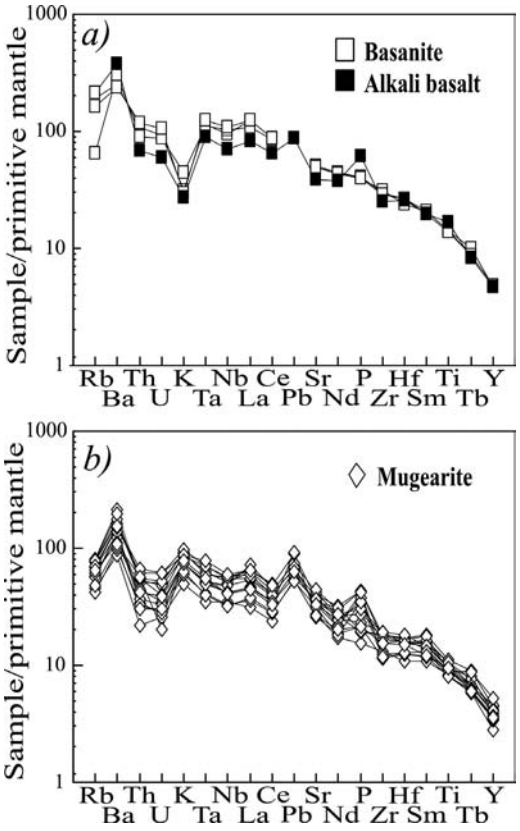

Fig. 5 – Primitive-mantle normalised diagrams for representative Montiferro basanites and alkali basalts (a) and mugearites (b). Normalisation values from Sun and McDonough (1989).

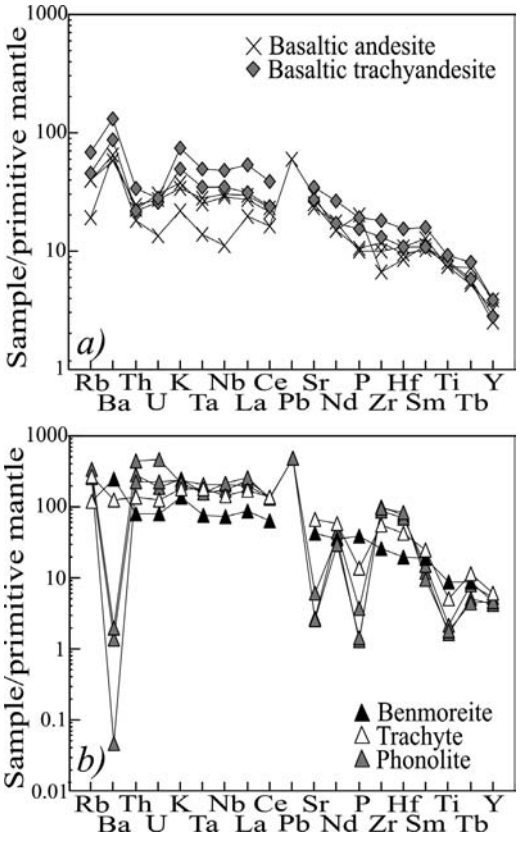

Fig. 6 – Primitive-mantle normalised diagrams for representative Montiferro basaltic andesites and basaltic trachyandesites (a) and benmoreites, trachytes and phonolites (b). Normalisation values from Sun and McDonough (1989).

Ba) enrichments, coupled with a slight negative K peak. LREE are enriched with respect to both MREE [e.g., $(La/Sm)_N$ ~4-6, where the subscript "*N*" stays for "chondrite-normalised", after Sun and Mc Donough (1989)] and HREE [e.g., $(La/Yb)_N$ ~30]. These rocks have no or very small Eu negative anomalies, with Eu/Eu* clustering between 0.9 and 1.1 [$Eu/Eu^* = Eu_N/(Sm_N*Gd_N)^{1/2}$] and show slight LILE (Large Ion Lithophile Elements) vs. HFSE enrichment, with Ba/Zr within the range 8.3-15. Mugearites show similar patterns, with positive peaks at Ba, Pb and P, and a slight negative Th peak (Fig. 5). With respect to Montiferro primitive samples, mugearites are less enriched in incompatible elements and LREE [e.g., $(La/Yb)_N$ ~14-28, $(La/Sm)_N$ ~2.8-4.3]. Basaltic andesites also show similar patterns (Fig. 6), with even lower incompatible elements enrichment and lower LREE/HREE [i.e., $(La/Yb)_N$ ~9-13.5] and LILE/HFSE [i.e., Ba/Zr ~5.5-9.9] ratios. Benmoreites have patterns quite similar to those of less evolved products (Fig. 6), with slightly different enrichment factors [e.g., $(La/Yb)_N$ ~28, $(La/Sm)_N$ ~4.5]. Trachytes and phonolites are characterised by higher incompatible element abundances and by strongly spiked patterns, with

Table 7

*Trace elements (ppm; analyzed by ICP-MS), $^{87}Sr/^{86}Sr$ and $^{143}Nd/^{144}Nd$ of representative Montiferro samples (*Lustrino *et al.*, 2007a*). b.d.l. = below detection limit; n.d. = not determined. Rock acronyms as in Table 6*

Label	GFP44	GFP51	GFP64	FDP48	GFP69	GFP83	GFP84	GFP92	GFP95	FDP11	FDP14	FDP18	FDP21
Unit	UAB	UAB	UAB	LAB	BD	BD	BD	BD	BD	BD	BD	BD	BD
Rock type (TAS)	Bsn	Bsn	Bsn	AB	Mug	Mug	Mug	Mug	Mug	Mug	Mug	Mug	Mug
La	85.1	75.4	85.5	56.8	44.4	38.1	43.3	44.5	49.4	31.9	41.4	24.7	45.1
Ce	157.0	150.2	155.8	113.8	88.7	73.1	76.2	86.3	81.1	62.4	71.6	49.6	85.6
Pr	18.0	16.9	17.8	13.3	10.8	8.7	9.2	10.3	10.6	7.5	8.5	6.1	9.7
Nd	59.9	60.4	58.5	50.5	43.0	33.7	36.1	39.8	42.0	29.7	33.0	25.2	36.7
Sm	9.1	9.3	8.8	8.7	8.0	6.5	6.9	7.2	7.9	5.9	6.2	5.4	6.6
Eu	2.8	2.9	2.7	2.6	2.7	2.1	2.2	2.4	2.4	1.9	2.0	1.9	2.1
Gd	6.6	10.9	6.5	6.7	8.5	5.2	5.7	7.5	6.7	4.8	5.0	4.7	5.0
Tb	0.9	1.1	0.9	0.9	1.0	0.7	0.7	0.8	1.0	0.7	0.7	0.7	0.7
Dy	4.9	5.5	4.9	4.6	4.9	3.7	3.9	4.3	4.9	3.4	3.8	3.5	3.4
Ho	0.8	0.9	0.8	0.8	0.8	0.6	0.7	0.7	0.9	0.6	0.6	0.6	0.6
Er	2.1	2.2	2.0	1.9	1.9	1.6	1.6	1.8	2.0	1.4	1.6	1.5	1.3
Tm	0.3	0.3	0.3	0.3	0.2	0.2	0.2	0.2	0.3	0.2	0.2	0.2	0.2
Yb	1.7	1.7	1.8	1.5	1.4	1.3	1.2	1.4	1.5	1.1	1.4	1.2	1.1
Lu	0.3	0.2	0.3	0.2	0.2	0.2	0.2	0.2	0.2	0.2	0.2	0.2	0.2
Hf	8.2	7.4	8.2	8.0	5.3	4.8	4.7	4.8	5.2	4.0	5.0	3.8	5.5
Ta	4.7	4.6	5.1	3.7	2.5	2.9	2.6	2.4	2.2	2.1	2.9	1.7	3.2
Pb	b.d.l.	b.d.l.	b.d.l.	6.2	b.d.l.	4.8	5.3	b.d.l.	b.d.l.	4.1	4.9	3.8	6.3
Th	9.2	7.6	9.9	5.8	4.3	4.5	4.7	4.7	3.7	3.1	5.2	2.8	5.6
U	1.9	1.8	2.2	1.3	1.1	1.0	0.8	1.1	0.7	0.7	1.3	0.6	1.3
$^{87}Sr/^{86}Sr$	n.d.	0.70434	n.d.	n.d.	0.70470	n.d.	n.d.	0.70474	0.70463	n.d.	n.d.	n.d.	n.d.
$^{143}Nd/^{144}Nd$	n.d.	0.51259	n.d.	n.d.	0.51247	n.d.	n.d.	n.d.	0.51244	n.d.	n.d.	n.d.	n.d.

strong negative anomalies at Ba, Sr, P, Eu and Ti (Fig. 6), very likely due to fractionation effects.

Sr and Nd isotopic compositions

Eleven representative Montiferro samples were analyzed for Sr and Nd isotopic ratios. $^{87}Sr/^{86}Sr$ shows a relatively narrow range, from 0.70434 to 0.70502 (Table 7), with the exception of one phonolitic sample (GFP52) showing very radiogenic composition ($^{87}Sr/^{86}Sr$ = 0.70739). Notwithstanding the narrow range of $^{87}Sr/^{86}Sr$ ratios, a negative correlation between $^{87}Sr/^{86}Sr$ and MgO can be observed. $^{143}Nd/^{144}Nd$ ranges from 0.51259 to 0.51244 and positively correlates with MgO.

In Fig. 7, isotopic data of the Montiferro samples are plotted together with other Sardinian Middle Miocene-Quaternary volcanic rocks. On the basis of isotopic and trace element data, these samples were formerly subdivided in two groups: the RPV (Radiogenic Pb Volcanics) and UPV (Unradiogenic Pb Volcanics; Lustrino *et al.* 2000, 2004, 2007a). The RPV comprises the rare and oldest volcanic rocks (~11.8-4.4 Ma) outcropping exclusively in the southern sector of Sardinia (Isola del Toro, Capo Ferrato, Guspini and Rio Girone), whereas the UPV group comprises more than 99% of the outcrops, emplaced between 3.9 and ~0.1 Ma (Lustrino *et al.*, 2007a, 2007b) throughout central and northern Sardinia. Montiferro samples fall well within the field of the UPV group, again with the only exception of phonolite GFP52 (Fig. 7).

TABLE 7 — *continued...*

FDP38	FDP40	FDP60	GFP57	GFP89	GFP42	GFP52	GFP85	GFP54	GFP55	FDP57	GFP49	GFP59	Label
BD	BD	BD	BD	TP	TP	TP	TP	BD	BD	BD	BD	BD	Unit
Mug	Mug	Mug	Ben	T	P	P	P	bA	bA	bA	bTA	bTA	Rock type (TAS)
25.9	31.4	30.1	59.8	116.9	160.7	136.3	179.3	18.7	20.4	13.7	21.7	36.9	La
51.0	61.4	58.5	113.8	246.6	239.5	242.3	230.9	38.0	41.5	29.3	42.7	69.0	Ce
6.2	7.3	6.9	13.2	23.8	19.8	22.2	16.8	5.0	5.5	4.2	5.6	9.1	Pr
24.9	29.2	27.2	48.5	78.9	51.1	60.9	40.1	20.6	23.7	20.1	23.2	36.2	Nd
5.2	5.9	5.4	8.4	11.0	5.4	6.7	4.3	4.6	5.6	5.0	4.9	7.0	Sm
1.8	1.9	1.8	2.7	3.2	1.2	1.1	0.7	1.5	1.9	1.8	1.6	2.2	Eu
4.4	4.9	4.5	8.8	12.1	3.9	10.1	3.4	4.5	5.3	4.2	4.7	6.7	Gd
0.6	0.7	0.6	0.9	1.2	0.5	0.9	0.5	0.6	0.8	0.6	0.6	0.9	Tb
3.4	3.5	3.4	4.8	6.4	3.1	4.9	2.9	3.1	4.2	3.0	3.4	4.4	Dy
0.6	0.6	0.6	0.8	1.0	0.6	0.8	0.6	0.5	0.7	0.5	0.6	0.7	Ho
1.5	1.5	1.5	1.9	2.8	1.9	2.6	2.0	1.3	1.7	1.3	1.4	1.7	Er
0.2	0.2	0.2	0.2	0.4	0.3	0.4	0.4	0.2	0.2	0.2	0.2	0.2	Tm
1.2	1.2	1.2	1.5	2.4	2.3	2.8	2.6	0.9	1.4	1.0	1.1	1.3	Yb
0.2	0.2	0.2	0.2	0.3	0.4	0.4	0.4	0.1	0.2	0.1	0.1	0.2	Lu
3.9	4.0	4.7	6.1	13.3	23.7	22.0	25.9	2.9	3.4	2.6	3.3	4.7	Hf
1.7	2.1	2.3	3.1	7.5	6.5	8.3	6.5	1.0	1.1	0.6	1.4	2.0	Ta
3.8	4.4	6.6	b.d.l.	b.d.l.	35.1	b.d.l.	34.3	b.d.l.	b.d.l.	4.2	b.d.l.	b.d.l.	Pb
2.6	3.6	4.8	6.8	11.7	23.7	19.3	37.3	1.9	2.1	1.6	1.9	2.9	Th
0.6	0.8	0.4	1.6	2.7	4.0	4.6	9.6	0.6	0.6	0.3	0.5	0.6	U
n.d.	n.d.	n.d.	0.70483	0.70502	n.d.	0.70739	n.d.	0.70443	0.70439	n.d.	0.70434	0.70458	$^{87}Sr/^{86}Sr$
n.d.	n.d.	n.d.	0.51244	0.51246	n.d.	0.51245	n.d.	0.51255	0.51253	n.d.	0.51256	0.51247	$^{143}Nd/^{144}Nd$

DISCUSSION

The magmatic evolution of Montiferro alkaline rocks

One of the main tasks regarding the magmatic evolution of Montiferro is to identify a possible genetic link within the alkaline products and between the alkaline and tholeiitic rocks. Among the alkaline rocks, representing the bulk of the complex, the variable degree of silica-undersaturation suggests the existence of two alkaline suites: a strongly alkaline series (starting from basanitic parental magmas and possibly reaching phonolitic compositions) and a mildly alkaline one (likely including alkali basalts, hawaiites, mugearites, benmoreites and trachytes). The only alkali basalt sample of this study (sample FDP48) appears to have major and trace elements composition more akin to basanites (Fig. 5). This sample is considered as a basanite whose degree of Si-undersaturation was apparently lowered by strong alteration resulting in a substantial alkali loss, as suggested by relatively high LOI values (3.55 wt.%; Table 6). Consequently, the only available products that could represent the less evolved terms of the mildly alkaline series are the hawaiites.

It is worth noting here that the widespread occurrence of analcite crystals in Montiferro alkaline rocks (especially the basanites) is a very interesting matter of debate. Di Battistini *et al.* (1990) extensively discussed this aspect and finally argued for a secondary origin of Montiferro analcite. Given that leucite is the

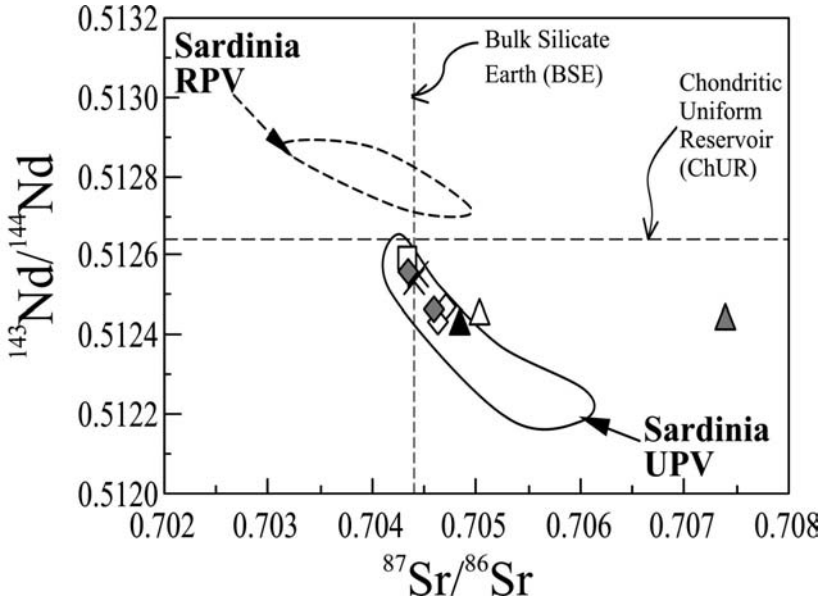

Fig. 7 – $^{143}Nd/^{144}Nd$ vs. $^{87}Sr/^{86}Sr$ diagram for the Montiferro samples. The fields of Sardinia UPV and RPV rocks (respectively, Unradiogenic Pb Volcanics and Radiogenic Pb Volcanics; Lustrino *et al.*, 2000; 2004; 2007a) are also reported. Literature data from Lustrino *et al.* (2000, 2002, 2007a), Gasperini *et al.* (2000). Symbols as in Fig. 2.

most likely primary phase to be replaced by secondary analcite, the primary sodic character of Montiferro alkaline rocks seems to be somewhat debatable. Leucite crystals are typical of potassic alkaline series, whose products have never been reported for the Middle Miocene-Quaternary volcanism of Sardinia. A possible further clue suggesting a primary potassic character of Montiferro alkaline rocks can be taken from the occurrence of biotite, both as phenocrysts and as megacrysts, in LAB basanites. A detailed treatment of the origin of analcite and of its petrological implications is, though intriguing, out of the scopes of this paper. Consequently, the primary sodic character of Montiferro alkaline rocks will not

Table 8

Major elements mass-balance calculations for the Montiferro alkaline rocks. Rock acronyms as in Fig. 2. Ol%, Pl%, Cpx%, Kfs%, Mt%, Ap% are the wt% of fractionating olivine, plagioclase, clinopyroxene, K-feldspar, magnetite and apatite, respectively. F% = wt.% of residual liquid; C% = wt.% of fractionating cumulate; ΣR^2 = sum of square residuals. Haw-P (calc) refers to the transition from hawaiite to phonolite obtained as a sum of the "intermediate" transitions. See text for further explanations

Transition	Ol%	Pl%	Cpx%	Kfs%	Mt%	Ap%	F%	C%	ΣR^2
Haw-Mug	18.2	51.1	24.0		6.7		74.3	25.7	0.039
Mug-Ben	17.5	36.4	35.0		11.1		71.0	29.0	0.148
Ben-T	13.2	27.5	38.1		15.7	5.5	75.3	24.8	0.814
T-P		28.1	5.5	58.2	7.5	0.8	44.6	55.4	0.205
Haw-P	12.8	41.1	20.4	15.6	8.4	1.7	11.1	88.9	0.166
Haw-P (calc)	12.3	37.3	24.2	15.6	9.5	1.1	17.7	82.3	

be debated here, but it will be tested in much more detail in a forthcoming paper.

In order to test the possible cogenetic character of Montiferro alkaline rocks, mass-balance calculations were performed. First of all, the possible recognition of all the terms belonging to a strongly alkaline series was tested. The composition of the most primitive magma was represented, alternatively, by the basanite GFP44 and by the alkali basalt FDP48 (considered to be akin to basanites, as discussed above). Starting from these samples, the transition from basanites to possible intermediate (i.e., hawaiites and mugearites) and evolved lithotypes (i.e., phonolites) was tested, but none of the performed calculations yielded acceptable results.

Regarding the mildly alkaline series, the transition from the least evolved to the most evolved rocks was subdivided into four steps: (1) from hawaiites (GFP73) to mugearites (GFP92); (2) from mugearites (GFP92) to benmoreites (FDP44); (3) from benmoreites (FDP44) to trachytes (GFP89); (4) from trachytes (GFP89) to phonolites (GFP52). Results are summarised in Table 8. Transition (1) was successfully modelled (i.e., ΣR^2 ~0.04; ΣR^2 = sum of the square of residuals) with a fractionation of 25% of an assemblage made up of labradorite (51%), salite (24%), olivine (18%) and Ti-magnetite (7%). Transition (2) was modelled with a fractionation of ~30% of andesine (37%), augite (35%), olivine (17%) and Ti-magnetite (11%), with ΣR^2 ~0.15. The third evolutionary step resulted into a fractionation of ~25% of a cumulate of augite (38%), andesine (27%), Ti-magnetite (17%), olivine (13%) and apatite (5%), with barely acceptable ΣR^2 values (i.e., ΣR^2 ~0.81). Finally, transition (4) was successfully modelled (ΣR^2 ~0.21) assuming a fractionation of ~55% of sanidine (58%), andesine (28%), Ti-magnetite (8%), salite (5%), and apatite (1%).

The sum of the above four "intermediate" evolutionary steps results in a transition from hawaiites to phonolites, which involves a fractionation of ~82% of a cumulate made of plagioclase (37%), clinopyroxene (24%), K-feldspar (16%), olivine (12%), Ti-magnetite (10%) and apatite (1%). This is in good agreement with the results of the direct modelling of the hawaiite-phonolite transition (Table 8). The close correspondence between the two models is a good confirmation of the overall reliability of the proposed evolutionary processes.

Similar modellings were performed by means of trace elements concentrations for each of the above mentioned evolutionary steps (see Appendix). For each evolutionary step, *calculated* C_l values ($C_l$calc) were compared with corresponding *observed* C_l values ($C_l$obs; i.e., the concentrations of a given trace element in the final term of the transition), revealing an overall good correspondence (Table 9). The results of trace elements modellings represent a substantial confirmation for the above fractional crystallisation modellings based on major-element calculations.

TABLE 9

Trace elements modellings for the evolution of the Montiferro alkaline rocks. Rock acronyms as in Fig. 2. C_0 = trace element concentration in the least evolved magma; $C_l$obs = observed trace element concentration in the most evolved magma; $C_l$calc = calculated trace element concentration in the most evolved magma. See text and appendix for further explanations

Haw-Mug transition				Mug-Ben transition			
	C_0	$C_l$obs	$C_l$calc		C_0	$C_l$obs	$C_l$calc
Zn	93	101	104	Zn	101	82	91
Ni	186	118	112	Ni	118	61	53
Rb	45	50	58	Rb	50	70	67
Sr	793	925	853	Sr	925	753	737
Y	35	16	45	Y	16	18	20
Zr	194	190	249	Zr	190	222	251
Nb	38	37	41	Nb	37	38	38
Sc	19	18	18	Sc	18	7	7
V	183	185	186	V	185	128	123
Cr	274	182	152	Cr	182	73	62
Ba	1169	1384	1260	Ba	1384	1385	1422
Ben-T transition				**T-P transition**			
	C_0	$C_l$obs	$C_l$calc		C_0	$C_l$obs	$C_l$calc
Ni	61	1	19				
Rb	70	168	91	Rb	168	164	196
Sr	753	1391	911	Sr	1396	57	6
Y	18	26	16	Y	26	28	47
Zr	222	611	287	Zr	611	966	1260
Nb	38	94	48	Nb	94	120	202
Sc	7	4	3	Sc	4	2	5
V	128	45	17	V	45	24	6
Ba	1385	884	904	Ba	884		

The magmatic evolution of Montiferro subalkaline rocks

As for the alkaline rocks, the possible existence of a genetic link between Montiferro subalkaline rocks (i.e., few basaltic andesites and qz-normative basaltic trachyandesites), was tested by means of mass-balance calculations. The transition from the least evolved basaltic andesite sample (GFP54) to the most evolved qz-normative basaltic trachyandesite sample (GFP53) was quite adequately modelled (ΣR^2 ~0.77) assuming the fractionation of ~28% of an assemblage made of labradorite (38%), olivine (28%), augite (17%) and orthopyroxene (17%). Results are reported in Table 10.

Modellings of the magmatic evolution of Montiferro subalkaline vulcanites were also performed by means of trace elements concentrations. Again, the good overall correspondence between calculated and observed C_l values is taken as a confirmation of the reliability of the proposed model (Table 10).

Table 10

Major- and trace elements modellings for the evolution of the Montiferro subalkaline rocks. Rock acronyms as in Fig. 2. Ol%, Pl%, Cpx%, Opx% are the wt% of fractionating olivine, plagioclase, clinopyroxene and orthopyroxene, respectively. Abbreviations and further indications on the performed models as reported in Table 8 and Table 9

Transition	Ol%	Pl%	Cpx%	Opx	F%	C%	ΣR^2
bA-bTA	27.9	16.9	38.0	17.2	71.6	28.4	0.766
	C_0	$C_l$obs	$C_l$calc				
Zn	107	129	124				
Ni	148	122	119				
Rb	25	32	34				
Sr	533	661	606				
Y	19	20	25				
Zr	133	172	180				
Nb	21	27	29				
Sc	16	16	16				
V	161	163	163				
Cr	243	225	238				
Ba	451	665	605				

The sources of Montiferro magmas

The occurrence of both tholeiitic and Na-alkaline rocks is a very common feature within the Middle Miocene-Quaternary districts of Sardinia (Lustrino *et al.*, 2007a and references therein). The presence of two different rock series in the same volcanic district is possibly related to compositional heterogeneities within the source region or different degrees of partial melting of the same mantle source. In order to understand which of the two hypotheses is the most likely to explain the proposed case study, a comparison between the less evolved products of each of the occurring magmatic suites is, therefore, necessary.

The less evolved terms of the three recognised series are represented by basanites (strongly alkaline series), hawaiites/mugearites (mildly alkaline series) and basaltic andesites/basaltic trachyandesites (tholeiitic series). A first-order comparison between them could be taken from the primitive mantle-normalised patterns (Figs. 5-6), which show very similar trends with the only notable differences being related to different incompatible elements enrichment factors, progressively decreasing moving from basanites to hawaiites to basaltic andesites. One should argue that, apart from the basanites, these samples can not be taken as representative of primary magmas compositions, given their relatively low Mg# [0.66-0.50, 0.63-0.55 and 0.73-0.65 for hawaiites/mugearites, basaltic andesites and basanites, respectively; Mg# = Mg/(Mg+Fe^{2+}), assuming Fe^{3+}/Fe^{2+} ratio = 0.15] and their low MgO, Cr and Ni contents (Table 6). Inter-elemental ratios between incompatible trace elements showing a roughly similar degree of incompatibility should have only very slightly modified in response to fractionation processes. Therefore, their values likely reflect those of the respective original primitive magmas. The general constancy of such inter-elemental ratios, shown by the linear trends of diagrams like Nd vs. Zr, Ta vs. Zr and Th vs. U (Fig. 8), strongly argues in favour of a common source for all the Montiferro rocks. The different

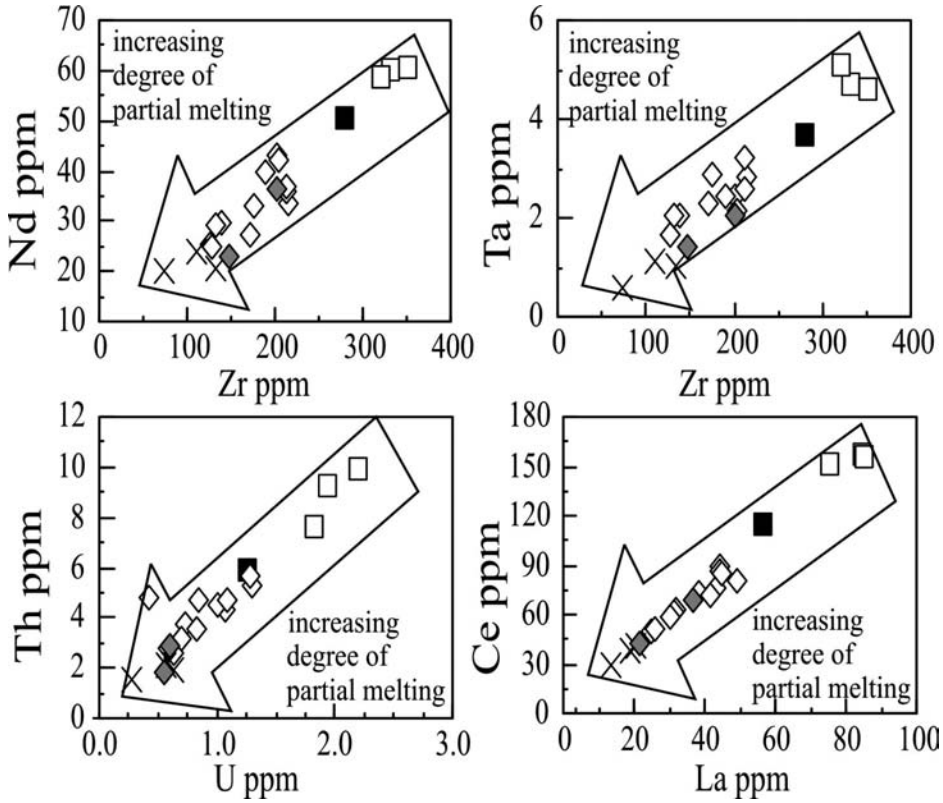

Fig. 8 – Interelemental ratios diagrams for the Montiferro samples. Symbols as in Fig. 2. The big arrows indicate the direction of the change in composition determined by an increase of the degree of partial melting of a generic mantle source. See text for further explanations.

incompatible trace element contents, therefore, is interpreted as reflecting different degrees of partial melting of the same mantle source, with the alkaline magmas (and particularly the basanites) originated from lower degrees of partial melting with respect to the tholeiitic ones (Fig. 8).

Assuming that all the Montiferro magmas come from a common mantle source, the subsequent step is to constrain the mineralogy of the source region. Possible mantle sources are represented by lherzolites equilibrated in garnet or spinel facies. Assuming a mantle source composition lying within the range of the lithospheric mantle estimates of McDonough (1990), the trace element compositions of magmas generated in the presence of a garnet-bearing and a spinel-bearing equilibrium assemblage were calculated (for different values of the degree of partial melting) by resolving Shaw's equation for equilibrium non modal batch melting for C_l. A detailed description of the performed partial melting calculations is given in the Appendix. Zr/Y vs. Zr and La/Yb vs. Zr diagrams (Fig. 9) seem to exclude a partial melting in presence of garnet as residual phase, because it would result into significantly higher Zr/Y and La/Yb; conversely, a spinel source seems more reasonable. The calculated melting trends of the proposed mantle source are not perfectly overlapping the trends depicted by Montiferro samples, as it is evident for example, from the La/

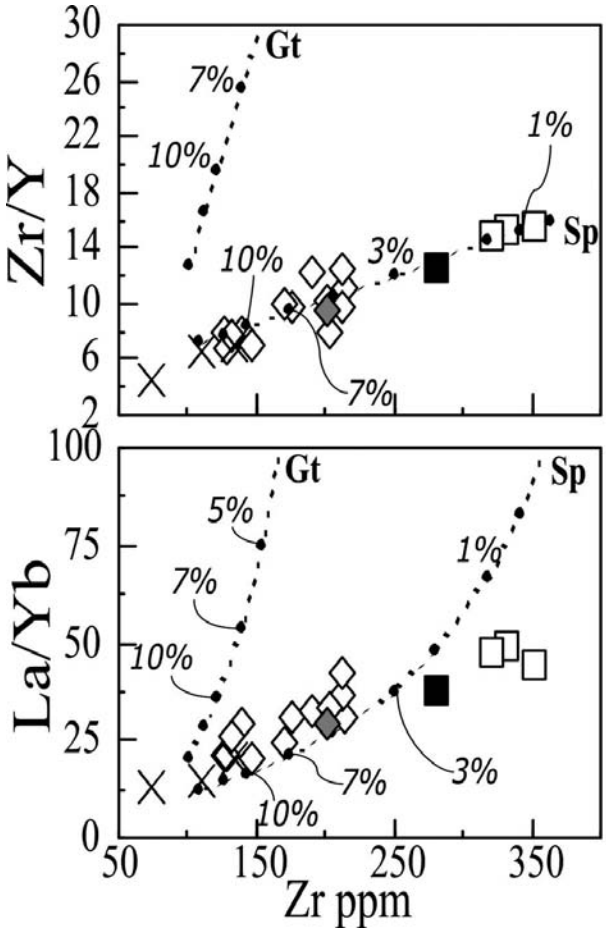

Fig. 9 – Zr/Y vs. Zr and La/Yb vs. Zr diagrams for the Montiferro samples. Symbols as in Fig. 2. The Gt and Sp broken lines represent, respectively, the calculated compositions of magmas generated by the partial melting of a garnet- (Gt) and a spinel- (Sp) bearing mantle source at given degrees of partial melting (% reported in italics). See text and Appendix for further explanations.

Yb vs. Zr diagram, where Montiferro rocks show slightly higher La/Yb values at a given Zr content. This could be due to the non-primitive character of the samples, particularly evident for the mildly alkaline and subalkaline products, which, therefore, could have reached higher La/Yb values just as a consequence of subsequent fractionation processes. A spinel-bearing mantle source was already proposed for other UPV Middle Miocene-Quaternary rocks from Sardinia, whose genesis has been ascribed to partial melting process taking place within the lithospheric mantle equilibrated in the spinel stability field (Lustrino *et al.*, 2002, 2004, 2007a). The calculated composition of the hypothetical magmas generated at given values of the degree of partial melting of the assumed mantle source were then normalised to chondritic estimates and plotted in Figs. 10-12 together with samples representing the possible primary magmas of the three series of the Montiferro complex. Again, primary magmas coming from a garnet-bearing peridotite strongly diverge from

the patterns of Montiferro rocks (Figs. 10a-11a-12a). On the other hand, magmas coming from a spinel-bearing peridotite more satisfactory represent the patterns of basanites and mugearites (Figs. 10b-11b), whereas the observed basaltic andesite pattern is more problematic (Fig. 12b). Basanites plot between magmas generated for degrees of partial melting of 1% and 3%, whereas mugearites fall between 5% and 7% and basaltic andesites between 10% and 12%. Values obtained for mugearites and basaltic andesites are possibly slight underestimates, given the non-primitive character of these rocks, as discussed above.

Crustal and mantle source contamination

Mantle-derived magmas may carry the evidences of various interactions with crustal components, which can take place in two basically different ways: assimilation of crustal lithologies by magmas *en route* to the surface and metasomatic interaction between mantle and crustal material within the mantle source region. The possible interaction between Montiferro mantle-derived melts and crust-derived melts, and the recognition of the exact nature of these processes were investigated by means of Sr-Nd isotopes.

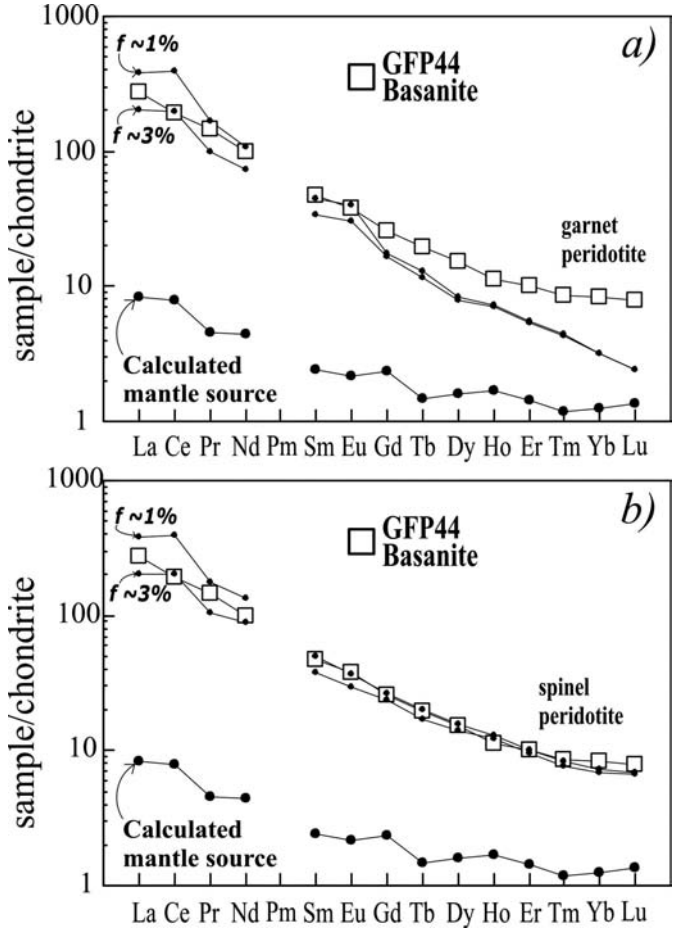

Fig. 10 – Chondrite-normalised [after Sun and McDonough (1989)] pattern of a representative Montiferro basanite sample. Also reported are the spidergram patterns relative to an hypothetical calculated mantle source and to magmas generated by a degree of partial melting (f) of ~1% and ~3% of this source equilibrated a) in the garnet and b) in the spinel stability field. See text and Appendix for further explanations.

As previously observed, Montiferro samples plot within the field of Sardinian UPV rocks in terms of $^{143}Nd/^{144}Nd$ and $^{87}Sr/^{86}Sr$, as well as Pb isotopic ratios. An origin from a lithospheric mantle source metasomatised after the interaction with lower crustal material in the source region was proposed for the UPV rocks by this research group (e.g., Lustrino *et al.*, 2007a and references therein), whereas the role of crustal contamination processes seems to be negligible. Several evidences were reported by Lustrino *et al.* (2007a) in support of this, such as the lack of any correlation between $^{87}Sr/^{86}Sr$ ratios and MgO contents (which excludes a major role for AFC processes), presence of large mantle xenoliths (whose diffuse occurrence is an evidence of quick magma uprise; Spera, 1987) and the positive correlation between $^{206}Pb/^{204}Pb$ and MgO. In contrast, Montiferro mafic rocks show a restricted range of $^{87}Sr/^{86}Sr$ ratios, positively correlating with the degree of rocks evolution. This can be interpreted as an evidence of limited involvement of crustal assimilation processes, further evidenced by the occurrence of large ultramafic mantle xenoliths. The only sample

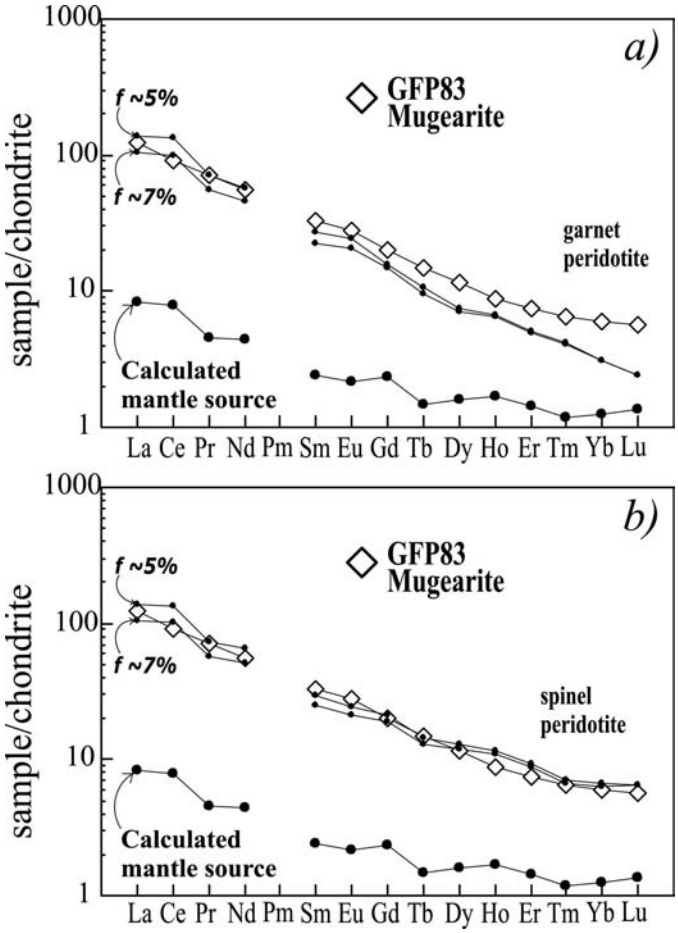

Fig. 11 – Chondrite-normalised [after Sun and McDonough (1989)] pattern of a representative Montiferro mugearite sample. Also reported are the spidergram patterns relative to an hypothetical calculated mantle source and to magmas generated by a degree of partial melting (f) of ~5% and ~7% of this source equilibrated a) in the garnet and b) in the spinel stability field. See text and Appendix for further explanations.

showing a significantly higher $^{87}Sr/^{86}Sr$ is the phonolite GFP52. This is probably due to a more intensive and prolonged interaction with crustal lithologies, possibly linked to higher residence times within crustal magma chambers, which could have also determined the highly evolved character of this sample.

As regards the possible causes of mantle source metasomatism, the most commonly invoked agent is represented by melts derived by partial meting of a lower crustal component (Lustrino *et al.*, 2000, 2004, 2007a; Lustrino, 2005), which resulted in an EMI-like geochemical signature (EMI = Enriched Mantle type I; e.g., Lustrino and Dallai, 2003). Lustrino *et al.* (2007a) proposed that this mantle metasomatism is a consequence of the delamination and detachment of ancient lower crustal portions, related to a Proterozoic collisional event. Typical evidences of a EMI-like mantle source, ascribed to the interaction between DMM-like source (DMM = Depleted MORB Mantle) and lower crustal components, are represented by low Nb/U, Ce/Pb and $^{206}Pb/^{204}Pb$, as well as slightly radiogenic $^{87}Sr/^{86}Sr$

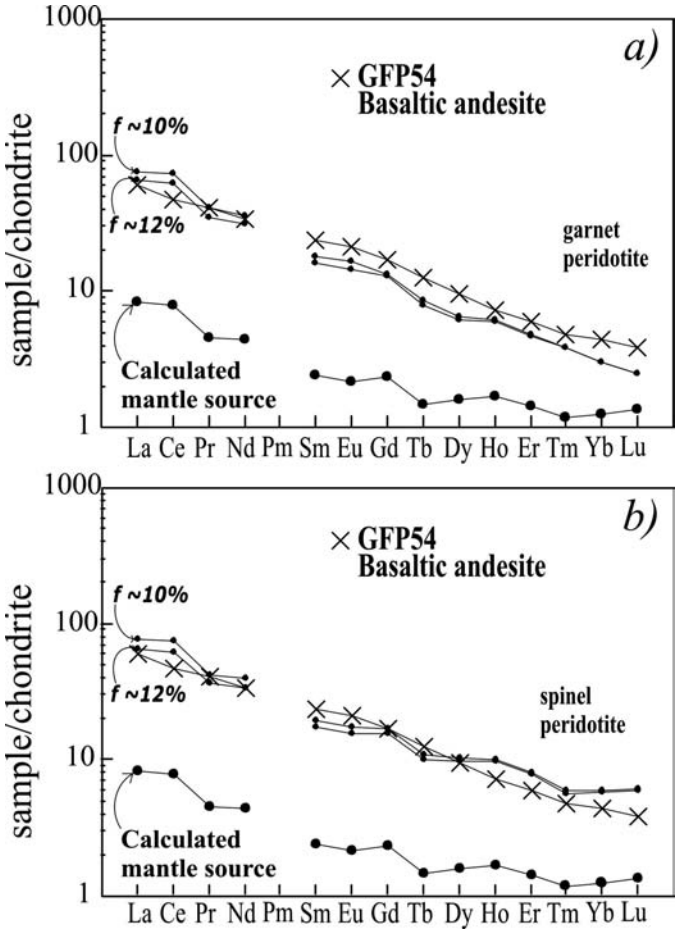

Fig. 12 – Chondrite-normalised [after Sun and McDonough (1989)] pattern of a representative Montiferro basaltic andesite sample. Also reported are the spidergram patterns relative to an hypothetical calculated mantle source and to magmas generated by a degree of partial melting (f) of ~10% and ~12% of this source equilibrated a) in the garnet and b) in the spinel stability field. See text and Appendix for further explanations.

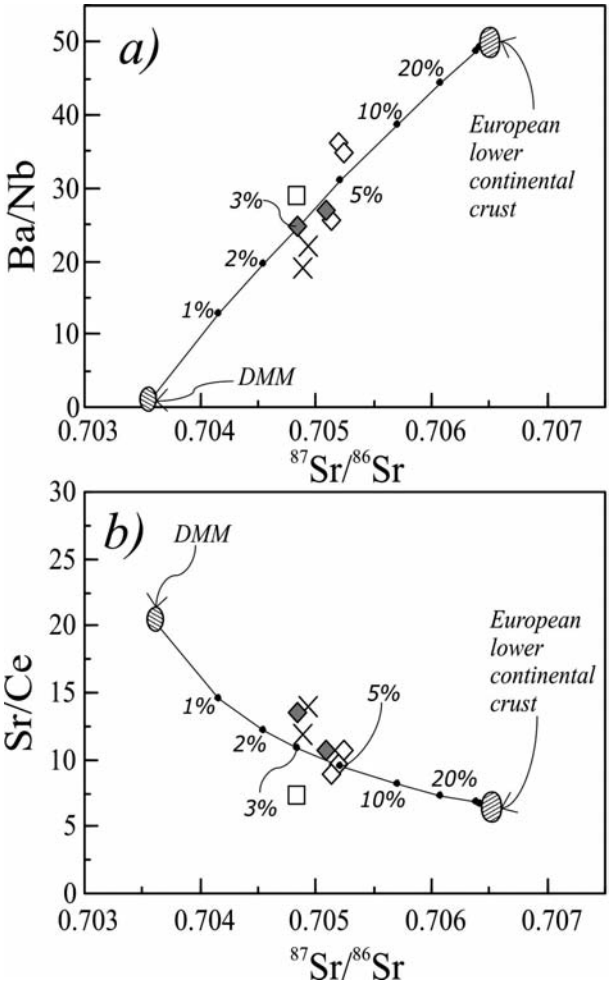

Fig. 13 – Ba/Nb vs. $^{87}Sr/^{86}Sr$ (a) and Sr/Ce vs. $^{87}Sr/^{86}Sr$ (b) diagrams for a selection of less evolved Montiferro samples. In both diagrams the mixing line between a DMM mantle component (McKenzie and O'Nions, 1995) and the average composition of European lower continental crust (Wedephol, 1995) are also shown. Numbers in italics indicate the percentages of the added lower crustal component. Symbols as in Fig. 2.

and highly unradiogenic $^{143}Nd/^{144}Nd$ values. A mixing curve between a DMM end-member and a lower crust end-member, represented by the average composition of European lower continental crust, is shown in Fig. 13. Despite some scattering of data, the Ba/Nb vs. $^{87}Sr/^{86}Sr$ diagram (Fig. 13a) shows that the Montiferro less evolved magmas are likely to have originated from a DMM-like source metasomatised by lower crustal rocks, whose abundances are between ~3 and ~7%. Slightly minor crustal involvement can be inferred from Sr/Ce vs. $^{87}Sr/^{86}Sr$ (Fig. 13b) and Ce/Ba vs. $^{87}Sr/^{86}Sr$ (not shown) diagrams, where the required quantity is around 3-5% (although with a general higher scatter of data).

Conclusions

The volcanic activity at Montiferro has occurred between 3.9 and 1.6 Ma, with a climax around 3.6 Ma, corresponding to the emplacement of the main trachytic-phonolitic body. Three magmatic series were recognised: (1) a strongly alkaline sodic series, represented by basanites with high silica-undersaturation, strong incompatible elements enrichment and high TiO_2 and Na_2O/K_2O; (2) a mildly alkaline sodic series, including hawaiites, mugearites (the main lithotypes), benmoreites, trachytes and phonolites, with the least evolved lithotypes ranging from silica-undersaturated to saturated and showing lower TiO_2, Na_2O/K_2O and incompatible trace elements contents with respect to their strongly alkaline counterparts; (3) a tholeiitic series, represented by minor basaltic andesites and basaltic trachyandesites, characterised by lower incompatible trace element contents with respect to the alkaline rocks. Substantially similar incompatible elements patterns and $^{87}Sr/^{86}Sr$ and $^{143}Nd/^{144}Nd$ isotope ratios suggest that the three series have generated from a common mantle source, likely represented by a spinel lherzolite. This mantle source resulted to consist of a DMM-like lithospheric mantle metasomatised by small additions of a lower crustal component, is likely to have experienced different degrees of partial melting in order to generate the strongly alkaline (f ~1-3%), mildly alkaline (f ~5-7%) and subalkaline (f ~10-12%) Montiferro primitive magmas.

A possible model for the volcanological-petrological evolution of the Montiferro complex can be drawn as follows.

1. Genesis of the basanitic magmas by very low degrees of partial melting and subsequent rapid upraise to the surface (as testified by the occurrence of ultramafic mantle xenoliths), which hampered substantial differentiation processes. Emplacement of the products of the LAB unit.

2. Genesis of alkaline and subordinate subalkaline magmas for different degrees of partial melting of the same source. The high volumes of alkaline magmas must have ponded in several crustal magma chambers, within which alkaline magmas differentiated reaching benmoreitic, trachytic and phonolitic compositions. Such evolved magmas were then erupted, possibly after slight interaction with crustal lithologies. The smaller volumes of the subalkaline magmas are not likely to have experienced intense differentiation processes and, therefore, were erupted only as basaltic andesites and basaltic trachyandesites. Emplacement of the TP unit.

3. The lower portions of the previously formed magma chambers, mainly consisting of less differentiated lithotypes (hawaiites and mugearites) were then erupted, together with smaller volumes of evolved products similar to those of the previous phase. Emplacement of the rocks of the BD unit.

4. Genesis of new basanitic magma batches, and subsequent eruption with no substantial differentiation. Emplacement of the products of the UAB unit.

Acknowledgements

The authors wish to thank Antonio Canzanella for assistance during XRF measurements, Vincenzo Monetti for the AAS analyses and Marcello Serracino for microprobe work. A. Montanini and L. Beccaluva are gratefully thanked for their constructive reviews. M.L. thanks William E. Cobham Jr. for Spectrum. This work has been supported by PRIN 2004 and FIRB 2001 grants (M.L. and V.M.).

Appendix

Trace elements modellings of Montiferro evolutionary processes were performed using Rayleigh's fractional crystallisation equation: $C_l/C_0 = F^{(D-1)}$. C_l is the concentration of a given trace element in the most evolved term of the transition; C_0 is the concentration of a given trace element in the least evolved term of the transition; F is the residual liquid fraction, whose values were derived from major elements modellings; D is the bulk partition coefficient, calculated as $D = \sum Kd_i * X_i$, where Kd_i is the partition coefficient of each of the crystallising phases for a specific trace element and X_i is the weight proportion of each crystallizing phase. X_i values are taken form major element modellings. Kd_i values for Montiferro alkaline rocks were taken from Nagasawa and Schnetzler (1971), Nagasawa (1973), Duke (1976), Okamoto (1979), Pedersen (1979), Luhr and Carmichael (1980), Dostal *et al.* (1983), Mahood and Hildreth (1983), Luhr *et al.* (1984), Nash and Crecraft (1985), Green and

Pearson (1987), Lemarchand *et al.* (1987), Bacon and Druitt (1988), Villemant (1988), McKenzie and O'Nions (1991), Nielsen *et al.* (1992), Hart and Dunn (1993), Bea *et al.* (1994), Dunn and Sen (1994), Ewart and Griffin (1994), Hauri *et al.* (1994), Morra *et al.* (2003). The substantial paucity of literature data on partition coefficients relative to phases in equilibrium with alkaline basic magmas has sometimes made necessary to use Kd_i determined for subalkaline primitive liquids. Kd_i values for Montiferro subalkaline rocks were taken from Ewart *et al.* (1973), Duke (1976), Dostal *et al.* (1983), McKenzie and O'Nions (1991), Hart and Dunn (1993), Dunn and Sen (1994), Hauri *et al.* (1994).

Partial melting calculations for the modelling of the mantle source of Montiferro magmas were performed using Shaw's equation for equilibrium non modal batch melting: $C_l/C_0 = 1/[D+f*(1-P)]$. C_l is the concentration of a given trace element in the primary magma; C_0 is the composition of a given trace element in the source; D is the bulk partition coefficient; P is the bulk partition coefficient during non-modal partial melting; f is the degree of partial melting. D was calculated as $\sum Kd_i*X_i$, where Kd_i is the partition coefficient of each of the residual source phases for a specific trace element and X_i is the weight proportion of each residual phase in the source; P as $\sum Kd_i*X_i$, where Kd_i is the partition coefficient of each of the phases entering in the melt for a specific trace element and X_i is the weight proportion of each of the phases entering in the melt. Kd_i values for D and P calculations were taken from Frey (1969), Matsui *et al.* (1977), Nicholls and Harris (1980), Villemant *et al.* (1981), Fujimaki *et al.* (1984), Irving and Frey (1984), McKenzie and O'Nions (1991), Hart and Dunn (1993), Hack *et al.* (1994), Hauri *et al.* (1994), Johnson (1994), Skulski *et al.* (1994). X_i values for D and P calculation were taken using the values reported in Kinzler and Grove (1992) for both garnet and the spinel mantle sources. For the garnet source the assumed ratios of X_{ol}:X_{opx}:X_{cpx}:X_{gt} in the source and as phases entering in the melt were 0.6:0.2:0.08:0.12 and 0.01:0.09:0.36:0.54, respectively. For the spinel source the assumed ratios of X_{ol}:X_{opx}:X_{cpx}:X_{sp} in the source and as phases entering in the melt were 0.57:0.28:0.13:0.02 and -0.06:0.28:0.67:0.11, respectively.

REFERENCES

Andersen D.J., Lindsley D.H., 1985. *New (and final) models for the Ti-magnetite/ilmenite geothermometer and oxygen barometer.* Eos, **66**, 416.

Assorgia A., Beccaluva L., Deriu M., Di Battistini G., Gallo F., Macciotta G., Pinali L., Venturelli G., Vernia L., Zerbi M. 1981. *Carta geopetrografica del complesso vulcanico del Montiferro (Sardegna centro-occidentale).* Grafiche STEP, Parma.

Assorgia A., Di Battistini G., Zerbi M., 1976. *Rocce basaltiche differenziate nel Montiferro sud-occidentale (Sardegna).* Ateneo Parm. Acta Nat., **12**, 135-175.

Assorgia A., Di Battistini G., Zerbi M., 1978. *Caratteri geopetrografici e vulcanologici del Montiferro meridionale (Tavv. Narbolia e S. Vero Milis), Sardegna.* Ateneo Parm. Acta Nat., **14**, 55-79.

Avanzinelli R., Boari E., Conticelli S., Francalanci L., Guarnirei L., Perini G., Petrone C.M., Tommasini S., Ulivi M., 2005. *High precision Sr, Nd, and Pb isotopic analyses using the new generation thermal ionisation mass spectrometer Thermofinnigan Triton-TI®.* Per Mineral, **74**, 147-166.

Bacon C.R., Druitt T.H., 1988. *Compositional evolution of the zoned calcalkaline magma chamber of Mt. Mazama, Crater Lake, Oregon.* Contrib. Mineral. Petrol., **98**, 224-256.

Bea F., Pereira M.D., Stroh A., 1994. *Mineral/leucosome trace-element partitioning in a peraluminous migmatite (a laser ablation-ICP-MS study).* Chem. Geol., **117**, 291-312.

Beccaluva L., Bianchini G., Bonadiman C., Coltorti M., Macciotta G., Siena F., Vaccaro C., 2005. *Within-plate cenozoic volcanism and lithospheric mantle evolution in the western-central mediterranean area.* In: Finetti I. (Ed.), Crop Project Deep Seismic exploration of the Central Mediterranean and Italy, Elsevier, 641-664.

Beccaluva L., Bianchini G., Coltorti M., Perkins W.T., Siena F., Vaccaro C., Wilson M., 2001. *Multistage evolution of the European lithospheric mantle: new evidence from Sardinian peridotite xenoliths.* Contrib. Mineral. Petrol., **142**, 284-297.

Beccaluva L., Bianchini G., Wilson M. (Eds.), 2007. *Cenozoic volcanism in the Mediterranean area.* Geol. Soc. Am. Spec. Publ., Bould.r, 358 pp.

Beccaluva L., Campredon R., Feraud G., Macciotta G., 1983. *Étude des relations entre volcanisme*

plio-quaternarie et tectonique en Sardigne à l'aide de l'analyse structurale des dykes. Bull. Volcanol., **46**, 365-379.

Beccaluva L., Civetta L., Macciotta G., Ricci C.A., 1985. *Geochronology in Sardinia: results and problems.* Rend. Soc. It. Min. Petr., **40**, 57-72.

Beccaluva L., Deriu M., Gallo F., Vernia L., 1973. *Le vulcaniti post-elveziane del Montiferro occidentale (Sardegna centro occidentale).* Mem. Soc. Geol. It., **12**, 1437-1457.

Beccaluva L., Deriu M., Maciotta G., Savelli C., Venturelli G., 1976-1977. *Geochronology and magmatic character of the Pliocene-Pleistocene volcanism in Sardinia (Italy).* Bull. Volcanol., **40**, 153-168.

Beccaluva L., Macciotta G., Venturelli G., 1975. *Dati geochimici e petrografici sulle vulcaniti Plio-Quaternarie della Sardegna centro-occidentale.* Boll. Soc. Geol. It., **94**, 1437-1457.

Brotzu P., Di Sabatino B., Morbidelli L., 1970a. *Contributo alla conoscenza delle vulcaniti post-elveziane del Montiferru. Nota VI. Distribuzione di alcuni elementi minori nella serie fonoliti-alcalibasalti del settore centrale del Montiferru (Sardegna centro-occidentale).* Per. Mineral., **39**, 19-49.

Brotzu P., Di Sabatino B., Morbidelli L., 1970b. *Contributo alla conoscenza delle vulcaniti post-elveziane del Montiferru. Nota VII. Caratteri mineralogici di un nodulo spinello-lherzolitico ospitato nelle lave basaltiche del settore di M. Urtigu.* Per. Mineral., **39**, 83-98.

Carminati E., Wortel M.J.R., Spakman W., Sabadini R., 1998. *The role of slab detachment processes in the opening of the western-central Mediterranean basin: some geological and geophysical evidence.* Earth Planet. Sci. Lett., **160**, 651-665.

Cioni R., Clocchiatti R., Di Paola G.M., Santacroce R., Tonarini S., 1982. *Miocene calcalkaline heritage in the Pliocene post-collisional volcanism of Monte Arci (Sardinia, Italy).* J. Volcanol. Geotherm. Res., **14**, 133-167.

Coulon C., Demant A., Bellon A., 1974. *Prémières datation par le methode K/Ar de quelques laves cénozoiques de la Sardaigne nord-occidentale.* Tectonophysics, **22**, 41-57.

Deriu M., 1952. *Contributo alla conoscenza delle manifestazioni vulcaniche della Sardegna centro e nord-occidentale. Nota II. Le rocce vulcaniche del settore di Santa Caterina di Pittinuri (Cuglieri).* Per. Mineral., **21**, 39-92.

Deriu M., 1954. *Biotite ed augite di Monte Columbargiu (Montiferru, Sardegna centro-occidentale).* Per. Mineral., **23**, 27-35.

Deriu M., Beccaluva L., Di Battistini G., Venturelli G., Zerbi M., 1974a. *I sistemi filoniani del Montiferro (Sardegna centro-occidentale).* Rend. Sem. Fac. Sci. Univ. Cagliari Vol. Monogr. "Paleogeografia del Terziario sardo nell'ambito del Mediterraneo occidentale", 171-212.

Deriu M., Di Battistini G., Gallo F., Giammetti F., Vernia L., Zerbi M., 1974b. *Caratteri geopetrografici del Montiferru centrale (Sardegna).* Mem. Soc. Geol. It., **13**, 415-439.

Di Battistini G., Montanini A., Zerbi M., 1990. *Geochemistry of volcanic rocks from southeastern Montiferro.* Jahrb. Miner. Abh., **162**, 35-67.

Dostal J., Dupuy C., Carron J.P., le Guen de Kerneizan, M., Maury R.C., 1983. *Partition coefficients of trace elements: application to volcanic rocks of St. Vincent, West Indies*. Geochim. Cosmochim. Acta, **37**, 525-533.

Duke J.M., 1976. *The distribution of the period for transition elements among olivine, calcic clinopyroxene and mafic silicate liquid*. J. Petrol., **17**, 499-521.

Dunn T., Sen C., 1994. *Mineral/matrix partition coefficients for orthopyroxene, plagioclase, and olivine in basaltic to andesitic systems: A combined analytical and experimental study*. Geochim. Cosmochim. Acta, **58**, 717-733.

Ewart A., Bryan W.B., Gill J., 1973. *Mineralogy and geochemistry of the younger volcanic islands of Tonga, S.W. Pacific*. J. Petrol., **14**, 429-465.

Ewart A., Griffin W.L., 1994. *Application of proton-microprobe data to trace-element partitioning in volcanic rocks*. Chem. Geol., **117**, 251-284.

Frey F.A., 1969. *Rare earth abundances in a high-temperature peridotite intrusion*. Geochim. Cosmochim. Acta, **33**, 1429-1447.

Fujimaki H., Tatsumoto M., Aoki K.-i., 1984. *Partition coefficients of Hf, Zr, and REE between phenocrysts and groundmasses*. J. Geophys. Res., **89**, 662-672.

Gallo F., Giammetti F., Vernia L., 1974. *Studio geopetrografico delle vulcaniti post-mioceniche del Montiferru nord-orientale (Sardegna).* Ateneo Parm. Acta Nat., **10**, 121-182.

Gasperini D., Blichert-Toft J., Bosch D., Del Moro A., Macera P., Télouk P., Albarede F., 2000. *Evidence from Sardinia basalt geochemistry for recycling of plume heads into the Earth's mantle.* Nature, **408**, 701-704.

Gelabert B., Sàbat F., Rodriguez-Perea A., 2002. *A new proposal for the late Cenozoic geodynamic evolution of the western Mediterranean.* Terra

Nova, **14**, 93-100.

Godano R.F., 2000. *Il magmatismo Plio-Quaternario Sardo. Correlazioni con l'evoluzione geodinamica della Sardegna*. Unpublished Ph.D. Thesis, Università degli Studi di Roma La Sapienza, 152 pp.

Green T.H., Pearson N.J., 1987. *An experimental study of Nb and Ta partitioning between Ti-rich minerals and silicate liquids at high pressure and temperature*. Geochim. Cosmochim. Acta, **51**, 55-62.

Gueguen E., Doglioni C., Fernandez M., 1998. *On the post-25 Ma geodynamic evolution of the western Mediterranean.* Tectonophysics, **298**, 259-269.

Hack P.J., Nielsen R.L., Johnston A.D., 1994. *Experimentally determined rare-earth element and Y partitioning behavior between clinopyroxene and basaltic liquids at pressures up to 20 kbar*. Chem. Geol., **117**, 89-105.

Hart S.R., Dunn T., 1993. *Experimental cpx/melt partitioning of 24 trace elements*. Contrib. Mineral. Petrol., **113**, 1-8.

Hauri E.H., Wagner T.P., Grove T.L., 1994. *Experimental and natural partitioning of Th, U, Pb and other trace elements between garnet, clinopyroxene and basaltic melts*. Chem. Geol., **117**, 149-166.

Irvine T.N., Baragar W.R.A., 1971. *A guide to the chemical classification of the common volcanic rocks*. Can. J. Earth Sci., **8**, 523-548.

Irving A.J., Frey F.A., 1984. *Trace element abundances in megacrysts and their host basalts: constraints on partition coefficients and megacryst genesis.* Geochim. Cosmochim, Acta, **48**, 1201-1221.

Johnson K.T.M., 1994. *Experimental cpx/ and garnet/ melt partitioning of REE and other trace elements at high pressures: petrogenetic implications*. Mineral. Mag., **58**, 454-455.

Kinzler R.J., Grove T.L., 1992. *Primary Magmas of Mid-Ocean Ridge Basalts 1. Experiments and Methods.* J. Geophys. Res., **97**, 6885-6906.

Langone A., Gueguen E., Prosser G., Caggianelli A., Rottura A., 2006. *The Curinga-Grifalco fault zone (northern Serre, Calabria) and its significance within the Alpine tectonic evolution of the western Mediterranean.* J. Geodyn., **42**, 140-158..

Le Bas M.J., Le Maitre R.W., Streckeisen A., Zanettin B., 1986. *A chemical classification of volcanic rocks based on the total alkali-silica diagram*. J. Petrol., **27**, 745-750.

Lecca L., Lonis R., Luxoro S., Melis E., Secchi F., Brotzu, P., 1997. *Oligo-Miocene volcanic sequences and rifting stages in Sardinia: a review*. Per Mineral., **66**, 7-61.

Lemarchand F., Benoit V., Calais G., 1987. *Trace element distribution coefficients in alkaline series*. Geochim. Cosmochim. Acta, **51**, 1071-1081.

Lindsley D.H., Spencer K.J., 1982. *Fe-Ti oxide geothermometry: Reducing analyses of coexisting Ti-magnetite (Mt) and ilmenite (I1m)*. Eos, **63**, 471.

Luhr J.F., Carmichael I.S.E., 1980. *The Colima Volcanic Complex, Mexico I. Post-caldera andesites from Volcan Colima*. Contrib. Mineral. Petrol., **71**, 343-372.

Luhr J.F., Carmichael I.S.E., Varekamp J.C., 1984. *The 1982 eruptions of El Chichon Volcano, Chiapas, Mexico: mineralogy and petrology of the anhydrite-bearing pumices*. J. Volcanol. Geotherm. Res., **23**, 69-108.

Lustrino M., 2000. *Petrogenesis of tholeiitic volcanic rocks from central-southern Sardinia*. Miner. Petrogr. Acta, 43, 1-16.

Lustrino M., 2005. *How the delamination and detachment of lower crust can influence basaltic magmatism*. Earth Sci. Rev., **72**, 21-38.

Lustrino M., Dallai L., 2003. *On the origin of the EM-I end-member.* N. Jahrb. Miner. Abh., **179**, 85-100.

Lustrino M., Melluso L., Morra V., 1999. *Origin of glass and its relationships with phlogopite in mantle xenoliths from central Sardinia (Italy).* Per. Mineral., **68**, 13-42.

Lustrino M., Melluso L., Morra V., 2000. *The role of lower continental crust and lithospheric mantle in the genesis of Plio-Pleistocene volcanic rocks from Sardinia (Italy).* Earth Planet. Sci. Lett., **180**, 259-270.

Lustrino M., Melluso L., Morra V., 2002. *The transition from alkaline to tholeiitic magmas: a case study from the Orosei-Dorgali Pliocene volcanic district (NE Sardinia, Italy).* Lithos, **63**, 83-113.

Lustrino M., Melluso L., Morra V., 2007a. *The geochemical uniqueness of "Plio-Quaternary" rocks of Sardinia in the circum-Mediterranean area.* In: Beccaluva L., Bianchini G., Wilson M. (Eds.), Cenozoic volcanism in the Mediterranean area, Geol. Soc. Am. Spec. Paper, **418**, 277-301.

Lustrino M., Melluso L., Morra V., Secchi F., 1996. *Petrology of Plio-Quaternary volcanic rocks from central Sardinia.* Per. Mineral., **65**, 275-287.

Lustrino M., Morra V., Fedele L., Serracino M., 2007b. *The transition between "orogenic"*

and "anorogenic" magmatism in the western Mediterranean area. The Middle Miocene volcanic rocks of Isola del Toro (SW Sardinia, Italy). Terra Nova, **19**, 148-159.

LUSTRINO M., MORRA V., MELLUSO L., BROTZU P., D'AMELIO F., FEDELE L., FRANCIOSI L., LONIS R., PETTERUTI LIEBERCKNECHT A.M., 2004. *The Cenozoic igneous activity of Sardinia*. Per. Mineral., **73**, 105-134.

LUSTRINO M., WILSON M., 2007. *The Circum-Mediterranean Anorogenic Cenozoic Igneous Province*. Earth Sci. Rev., **81**, 1-65.

MCDONOUGH W.F., 1990. *Constraints on the composition of the continental lithospheric mantle.* Earth Planet. Sci. Lett., **101**, 1-18.

MAHOOD G.A., HILDRETH E.W., 1983. *Large partition coefficients for trace elements in high-silica rhyolites*. Geochim. Cosmochim. Acta, **47**, 11-30.

MATSUI Y., ONUMA N., NAGASAWA H., HIGUCHI H., BANNO S., 1977. *Crystal structure control in trace element partition between crystal and magma*. Bull. Soc. Fr. Minéral. Cristallogr., **100**, 324-328.

MATTEI M., D'AGOSTINO N., FACCENNA C., PIROMALLO C., ROSSETTI F., 2004. *Some remarks on the geodynamics of the Italian region.* Per. Mineral., **73**, 7-27.

MCKENZIE D., O'NIONS R.K., 1991. *Paritial melt distributions from inversion of rare earth element concentrations*. J. Petrol., **32**, 1021-1091.

MCKENZIE D., O'NIONS R.K., 1995. *The source regions of Ocean Island Basalts.* J. Petrol., **36**, 133-159.

MELLUSO L., MORRA V., BROTZU P., RAZAFINIPARANY A., RATRIMO V., RAZAFIMAHATRATRA D., 1997. *Geochemistry and Sr-isotopic composition of the Cretaceous flood basalt sequence of northern Madagascar: petrogenetic and geodynamic implications*. J. Afr. Earth Sci., **24**, 371-390.

MONTANINI A., BARBIERI M., CASTORINA F., 1994. *The role of fractional crystallization, crustal melting and magma mixing in the petrogenesis of rhyolites and mafic inclusion-bearing dacites from the Monte Arci volcanic complex (Sardinia, Italy).* J. Volcanol. Geotherm. Res., **61**, 95-120.

MONTANINI A., HARLOV D., 2006. *Petrology and mineralogy of granulite-facies mafic xenoliths (Sardinia, Italy): Evidence for KCL metasomatism in the lower crust.* Lithos, **92**, 588-608.

MONTANINI A., ZERBI M., TOSCANI L., 1992. *Petrology of deep-seated spinel-rich gabbroic and pyroxenite xenoliths from Montiferro volcanic complex*. Miner. Petrogr. Acta, **25**, 77-98.

MORRA V., LUSTRINO M., MELLUSO L., RICCI G., VANNUCCI R., ZANETTI A., D'AMELIO F., 2003. *Trace element partition coefficients between feldspar, clinopyroxene, biotite, Ti-magnetite, apatite and felsic potassic glass from Campi Flegrei (S. Italy).* EGS-AGU-EUG Joint Assembly, Nice 2003 (abstract).

NAGASAWA H., 1973. *Rare-earth distribution in alkali rocks from Oki-Dogo Island, Japan*. Contrib. Mineral. Petrol., **39**, 301-308.

NAGASAWA H., SCHNETZLER C.C., 1971. *Partitioning of rare earth, alkali, and alkaline earth elements between phenocrysts and acidic igneous magmas*. Geochim. Cosmochim. Acta, **35**, 953-967.

NASH W.P., CRECRAFT H.R., 1985. *Partition coefficients for trace elements in silicic magmas*. Geochim. Cosmochim. Acta, **49**, 2309-2322.

NICHOLLS I.A., HARRIS K.L., 1980. *Experimental rare earth element partition coefficients for garnet, clinopyroxene and amphibole coexisting with andesitic and basaltic liquids*. Geochim. Cosmochim. Acta, **44**, 287-308.

NIELSEN R.L., GALLAHAN W.E., NEWBERGER F., 1992. *Experimentally determined mineral-melt partition coefficients for Sc, Y and REE for olivine, orthopyroxene, pigeonite, magnetite and ilmenite*. Contrib. Mineral. Petrol., **110**, 488-499.

OKAMOTO K., 1979. *Geochemical study on magmatic differentiation of Asama volcano, Central Japan*. J. Geol. Soc. Japan, **85**, 525-535.

PEDERSEN A.K., 1979. *Basaltic glass with high-temperature equilibrated immiscible sulphide bodies with native iron from Disko, Central West Greenland*. Contrib. Mineral. Petrol., **69**, 397-407.

RICOU L.E., 1994. *Thetys reconstructed: plates, continental fragments and their boundaries since 260 Ma from Central America to south-eastern Asia.* Geodin. Acta, **7**, 169-218.

ROEDER P.L., EMSLIE R.F., 1970. *Olivine-liquid equilibrium*. Contrib. Mineral. Petrol., **29**, 275-289.

ROSENBAUM G., LISTER G.S., DUBOZ C., 2002. *Reconstruction of the tectonic evolution of the western Mediterranean since the Oligocene.* J. Virtual Expl., **8**, 107-126.

SKULSKI T., MINARIK W., WATSON E.B., 1994. *High-pressure experimental trace-element partitioning between clinopyroxene and basaltic melts.* Chem. Geol., **117**, 127-147.

SPENCER K.J., LINDSLEY D.H., 1981. *A solution model for coexisting iron-titanium oxides.* Am. Mineral., **66**, 1189-1201.

SPERA F.J., 1987. *Tapping of melt by veins and dykes.*

J. Geophys. Res., **93**, 10255-10272.

Speranza F., Villa I.M., Cagnotti L., Florindo F., Cosentino D., Cipollari P., Mattei M., 2002. *Age of the Corsica-Sardinia rotation and Liguro-Provençal basin spreading: new paleomagnetic and Ar/Ar evidence.* Tectonophysics, **347**, 231-251.

Stormer J.C., 1983. *The effect of recalculation on estimates of temperature and oxygen fugacity from analyses of multicomponent iron-titanium oxides.* Am. Mineral., **68**, 586-594.

Sun S.S., McDonough W.F., 1989. *Chemical and isotopic systematics of oceanic basalts: implications for mantle compositions and processes.* In: Saunders A.D., Norry M.J. (Eds.), Magmatism in the Ocean Basins, Geol. Soc. Lond. Spec. Publ., **42**, 313-345.

Villemant B., 1988. *Trace element evolution in the Phlegrean Fields, Central Italy: fractional crystallization and selective enrichment.* Contrib. Mineral. Petrol., **98**, 169-183.

Villemant B., Jaffrezic H., Joran J.-L., Treuil M., 1981. *Distribution coefficients of major and trace elements; fractional crystallization in the alkali basalt series of Chaine des Puys (Massif Central, France).* Geochim. Cosmochim. Acta, **45**, 197-201

Wedepohl H., 1995. *Origin of the Tertiary basaltic volcanism in the northern Hessian depression.* Contrib. Mineral. Petrol., **89**, 122-143